Syntheses of Dinuclear and Trinuclear Hydridoplatinum Complexes with Bridging Phosphido Ligands $[Pt_2H_2(\mu\text{-}PR_2)_2(PEt_3)_2]$ (R = ^{t}Bu, Ph) and $[Pt_3H_2(\mu\text{-}PPh_2)_4(PEt_3)_2]$. Characterization of the Triangular Intermediate $[Pt_3H(\mu\text{-}PPh_2)_3(PEt_3)_3]$ and Its Chemical Properties

Masumi Itazaki, Yasushi Nishihara, and Kohtaro Osakada*

Chemical Resources Laboratory, Tokyo Institute of Technology, 4259 Nagatsuta, Midori-ku, Yokohama 226-8503, Japan

Received August 26, 2003

The reaction of Ph_2PH with $Pt(PEt_3)_3$ in 2:1 molar ratio produces the linear triplatinum complex $[Pt_3H_2(\mu\text{-}PPh_2)_4(PEt_3)_2]$ (**1**). X-ray crystallography of **1** shows the structure of the complex with two PEt_3 ligands at *anti* positions, while it exists as a mixture of the isomers with PEt_3 at *anti* and *syn* positions. $Pt(PEt_3)_3$ reacts with equimolar Ph_2PH to afford the dinuclear complex $[Pt_2H_2(\mu\text{-}PPh_2)_2(PEt_3)_2]$ (**2**) and the cyclic trinuclear complex $[Pt_3H(\mu\text{-}PPh_2)_3(PEt_3)_3]$ (**3**) depending on the reaction conditions. A dinuclear platinum(II) complex with a structure similar to **2**, $[Pt_2H_2(\mu\text{-}P^tBu_2)_2(PEt_3)_2]$ (**4**), is obtained by the reaction of ^{t}-Bu_2PH with $Pt(PEt_3)_3$. Isolated complexes **2** and **3** cleanly react with Ph_2PH to form **1**, indicating that the reaction of Ph_2PH with $Pt(PEt_3)_3$, giving **1**, involves these complexes as the intermediates. Complex **3** contains a triangular Pt_3 core with Pt−Pt bonds in the range 2.9784(4)−2.9983(3) Å, as shown by X-ray crystallography. The ^{1}H NMR spectrum of **3** exhibits the hydrido signal at δ −7.98 accompanied by splitting due to H−P and H−Pt coupling. Complex **3** reacts with Ph_3SiH and Ph_2SiH_2 to give silylplatinum complexes $[Pt_3(SiH_{n+1}Ph_{4-n})(\mu\text{-}PPh_2)_3(PEt_3)_2]$ (**5**, n = 1; **6**, n = 2). Cationic triangular complexes $[Pt_3(\mu\text{-}PPh_2)_3(PEt_3)_3]^+I^-$ (**7**) and $[Pt_3(\mu\text{-}PPh_2)_3(PEt_3)_3]^+[B_4O_4Ar_4(OH)]^-$ (**8**, Ar = C_6H_4Me-4; **9**, Ar = C_6H_4F-4; **10**, Ar = $C_6H_4CF_3$-4) are obtained from the reactions of complex **3** with MeI and with $ArB(OH)_2$, respectively.

Introduction

Bridging phosphido (μ-PR_2) ligands form a number of multimetallic complexes[1] of transition metals because of the stable coordination bond between the three-electron donor and the two metal centers. The M−P−M angles of the complexes vary ranging from 70° to 140°, depending on the presence or absence of the metal−metal bond between the metal centers and on the type of metal centers.[2] The flexible coordination of the phosphido ligand enables the binding of two transition metals of various homo-[3] and heterobimetallic[4] dinuclear complexes and cyclic trinuclear complexes of transition metals. There have been many reports of dinulclear and cyclic trinuclear platinum complexes with bridging phosphido ligands.[5−8] Triplatinum complexes with bridging phosphido ligands have three possible structures, shown in Scheme 1. The triangular

* Corresponding author. E-mail: kosakada@res.titech.ac.jp.

(1) (a) Bender, R.; Braunstein, P.; Dedieu, A.; Dusausoy, Y. *Angew. Chem.* **1989**, *101*, 931. (b) Schuh, W.; Wachtler, H.; Laschober, G.; Kopacka, H.; Wurst, K.; Peringer, P. *Chem. Commun.* **2000**, 1181. (c) Leoni, P, Marchetti, F.; Marchetti, L.; Pasquali, M.; Quaglierini, S. *Angew. Chem., Int. Ed.* **2001**, *40*, 3617.

(2) (a) Rosenberg, S.; Geoffroy, G. L.; Rheingold, A. L. *Organometallics* **1985**, *4*, 1184. (b) Brauer, D. J.; Hessler, G.; Knuppel, P. C.; Stelzer, O. *Inorg. Chem.* **1990**, *29*, 2370.

(3) Pd−Pd: (a) Hayter, R. G. *J. Am. Chem. Soc.* **1962**, *84*, 3046. (b) Alonso, E.; Forniés, J.; Fortuño, C.; Martín, A.; Rosair, G. M.; Welch, A. J. *Inorg. Chem.* **1997**, *36*, 4426. Ru−Ru: (c) Omori, H.; Suzuki, H.; Take, Y.; Moro-oka, Y. *Organometallics* **1989**, *8*, 2270.

(4) Zr (Hf)−Ni: (a) Baker, R. T.; Fultz, W. C.; Marder, T. B.; Williams, I. D. *Organometallics* **1990**, *9*, 2357. Pt−Mn (W): (b) Braunstein, P.; De Jesus, E.; Dedieu, A.; Lanfranchi, M.; Tiripicchio, A. *Inorg. Chem.* **1992**, *31*, 399. Pd−Pt: (c) Falvello, L. R.; Forniés, J.; Fortuño, C.; Martínez, F. *Inorg. Chem.* **1994**, *33*, 6242. Pt−Rh (Ir): (d) Falvello, L. R.; Forniés, J.; Martín, A.; Gomez, J.; Lalinde, E.; Moreno, M. T.; Sacristan, J. *Inorg. Chem.* **1999**, *38*, 3116. Au−Ag: (e) Blanco, M. C.; Fernandez, E. J.; Lopez-De-Luzuriaga, J. M.; Olmos, M. E.; Crespo, O.; Gimeno, M. C.; Laguna, A.; Jones, P. G. *Chem. Eur. J.* **2000**, *6*, 4116. Pt−Cu: (f) Archambault, C.; Bender, R.; Braunstein, P.; Dusausoy, Y. *Dalton Trans.* **2002**, 4084.

(5) μ-PPh_2: (a) Carty, A. J.; Hartstock, F.; Taylor, N. J. *Inorg. Chem.* **1982**, *21*, 1349. (b) Van Leeuwen, P. W. N. M.; Roobeek, C. F.; Frijns, J. H. G.; Orpen, A. G. *Organometallics* **1990**, *9*, 1211. (c) Alonso, E.; Casas, J. M.; Cotton, F. A.; Feng, X.; Forniés, J.; Fortuño, C.; Tomás, M. *Inorg. Chem.* **1999**, *38*, 5034. (d) Bender, R.; Bouaoud, S.-E.; Braunstein, P.; Dusausoy, Y.; Merabet, N.; Raya, J.; Rouag, D. *J. Chem. Soc., Dalton Trans.* **1999**, 735. (e) Falvello, L. R.; Forniés, J.; Gomez, J.; Lalinde, E.; Martín, A.; Moreno, M. T.; Sacristan, J. *Chem. Eur. J.* **1999**, *5*, 474.

(6) μ-P^tBu_2: (a) Leoni, P.; Pasquali, M.; Beringhelli, T.; D'Alfonso, G.; Minoja, A. P. *J. Organomet. Chem.* **1995**, *488*, 39. (b) Leoni, P.; Manetti, S.; Pasquali, M. *Inorg. Chem.* **1995**, *34*, 749, and references therein. (c) Leoni, P.; Pasquali, M.; Fortunelli, A.; Germano, G.; Albinati, A. *J. Am. Chem. Soc.* **1998**, *120*, 9564. (d) Leoni, P.; Pasquali, M.; Cittadini, V.; Fortunelli, A.; Selmi, M. *Inorg. Chem.* **1999**, *38*, 5257. (e) Leoni, P.; Chiaradonna, G.; Pasquali, M.; Marchetti, F. *Inorg. Chem.* **1999**, *38*, 253. (f) Cristofani, S.; Leoni, P.; Pasquali, M.; Eisentraeger, F.; Albinati, A. *Organometallics* **2000**, *19*, 4589. (g) Crementieri, S.; Leoni, P.; Marchetti, F.; Marchetti, L.; Pasquali, M. *Organometallics* **2002**, *21*, 2575.

10.1021/om034131v CCC: $27.50
Publication on Web 03/03/2004

Scheme 1

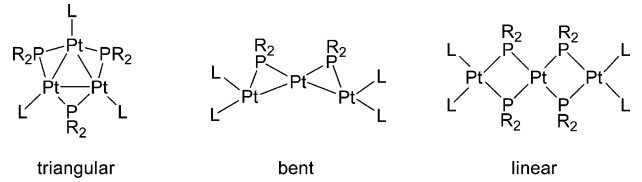

complexes with three Pt centers and three bridging phosphido ligands are most common among the three structures,[9,10] while the complexes with bent[11] and linear[12] structures were reported in a limited number of cases. The linear trinuclear platinum complexes with aryl and bridging phosphido ligands were prepared from mono- and dinuclear Pt complexes and from mono- and tetranuclear Pt complexes.[12]

In this paper, we report the preparation of a new linear triplatinum complex with hydrido and bridging phosphido ligands from the reaction of Ph_2PH with $Pt(PEt_3)_3$. The pathway of the reaction that involves an intermediate cyclic triplatinum complex and its reactions with organosilanes and arylboronic acids are also described.

Results and Discussion

The reaction of Ph_2PH with $Pt(PEt_3)_3$ in 2:1 molar ratio in benzene for 12 h and then in hexane for 96 h at room temperature gave the linear triplatinum(II) complex $[Pt_3H_2(\mu\text{-}PPh_2)_4(PEt_3)_2]$ (**1**) in 80% yield (eq 1).

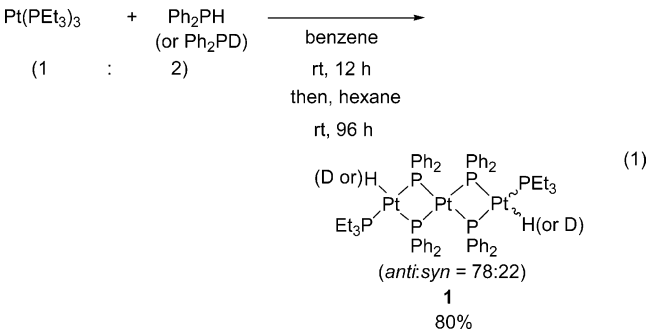

(1)

Figure 1 depicts the molecular structure of **1**·Me_2CO by X-ray crystallography. It consists of three square-planar Pt(II) centers, bridged by four μ-PPh_2 ligands. The two terminal Pt centers are bonded with a PEt_3 and two bridging PPh_2 ligands. The molecule has the PEt_3 ligands at the opposite side of the linear Pt−Pt−Pt alignment (*anti* position). The hydrido ligands are considered to occupy the vacant coordination sites of the square-planar Pt centers, although the positions of the hydrido ligands were not determined in the final D-map. The coordination planes around the terminal Pt atoms and that around the central Pt atom form an angle of 147.0°. The Pt···Pt distance of 3.572(1) Å strongly suggests the absence of an intermetallic bond. The Pt_2P_2 four-membered ring contains larger Pt−P−Pt bond angles (Pt(1)−P(2)−Pt(2) = 98.8(1)°, Pt(1)−P(3)−Pt(2) = 99.1(1)°) than the P−Pt−P bond angles (P(2)−Pt(1)−P(3) = 75.3(1)°, P(2)−Pt(2)−P(3) = 74.9(1)°).

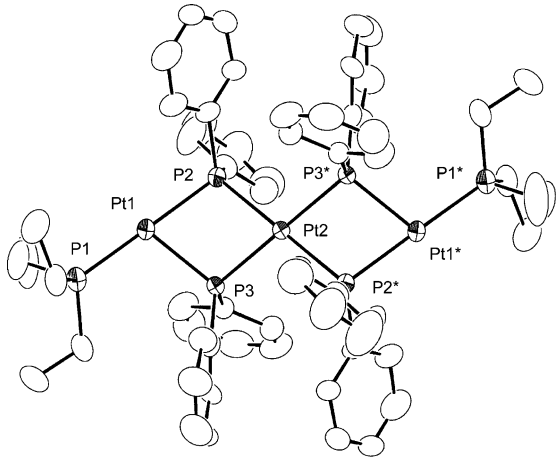

Figure 1. ORTEP drawing of *anti*-**1**·Me_2CO with 50% thermal ellipsoidal plots. Atoms with asterisks are crystallographically equivalent to those having the same number without asterisks. Hydrido ligands were not located. Hydrogen atoms and Me_2CO were omitted for simplicity. Selected bond distances (Å) and angles (deg): Pt(1)−P(1) = 2.277(4), Pt(1)−P(2) = 2.352(3), Pt(1)−P(3) = 2.336(4), Pt(2)−P(2) = 2.353(3), Pt(2)−P(3) = 2.357(3), Pt(1)···Pt(2) = 3.572(1), P(2)···P(3) = 2.865(5); P(1)−Pt(1)−P(2) = 178.0(2), P(1)−Pt(1)−P(3) = 105.3(1), P(2)−Pt(1)−P(3) = 75.3(1), P(2)−Pt(2)−P(3) = 74.9(1), Pt(1)−P(2)−Pt(2) = 98.8(1), Pt(1)−P(3)−Pt(2) = 99.1(1), P(2)−Pt(2)−P(2*) = 180.0, P(3)−Pt(2)−P(3*) = 180.0.

The ^1H NMR spectrum of **1** shows the hydrido signals at δ −5.83 (^2J(H−P) = 10, 22, 142 Hz, ^1J(H−Pt) = 1032 Hz) and δ −6.10 (^2J(H−P) = 11, 23, 142 Hz, ^1J(H−Pt) = 1036 Hz) in 78:22 peak area ratio. The two signals are attributed to the isomers having the hydrido ligands at *anti* or *syn* positions. We assigned the former signal to the structure with *anti* hydrides, which was characterized by X-ray crystallography. The signal at δ −6.10 with coupling constants similar to that at δ −5.83 is attributed to the isomer with *syn* structure. The reaction of Ph_2PD with $Pt(PEt_3)_3$ gives complex **1**-d_2, which shows broad ^2H NMR signals at δ −5.8 and −6.1 and no ^1H NMR signals in this region, indicating that the hydrido of the complex is derived from the P−H (or P−D) hydrogen of diphenylphosphine.

The $^{31}P\{^1H\}$ NMR spectrum of **1** contains the signals due to the major isomer with *anti* structure. The signals

(7) μ-PCy_2: Mastrorilli, P.; Nobile, C. F.; Cosimo, F.; Fanizzi, P.; Latronico, M.; Hu, C.; Englert, U. *Eur. J. Inorg. Chem.* **2002**, 1210.

(8) μ-PPhH: Parkin, I. P.; Slawin, A. M. Z.; Williams, D. J.; Woollins, J. D. *Inorg. Chim. Acta* **1990**, *172*, 159.

(9) μ-PPh_2: (a) Taylor, N. J.; Chieh, P. C.; Carty, A. J. *J. Chem. Soc., Chem. Commun.* **1975**, 448. (b) Bellon, P. L.; Ceriotti, A.; Demartin, F.; Longoni, G.; Heaton, B. T. *J. Chem. Soc., Dalton Trans.* **1982**, 1671. (c) Bender, R.; Braunstein, P.; Tiripicchio, A.; Camellini, M. T. *Angew. Chem., Int. Ed. Engl.* **1985**, *24*, 861. (d) Hadj-Bagheri, N.; Browning, J.; Dehghan, K.; Dixon, K. R.; Meanwell, N. J.; Vefghi, R. *J. Organomet. Chem.* **1990**, *396*, C47. (e) Bender, R.; Braunstein, P.; Dedieu, A.; Ellis, P. D.; Huggins, B.; Harvey, P. D.; Sappa, E.; Tiripicchio, A. *Inorg. Chem.* **1996**, *35*, 1223. (f) Bender, R.; Braunstein, P.; Bouaoud, S.-E.; Merabet, N.; Rouag, D.; Zanello, P.; Fontani, M. *New J. Chem.* **1999**, *23*, 1045. (g) Archambault, C.; Bender, R.; Braunstein, P.; Bouaoud, S.-E.; Rouag, D.; Golhen, S.; Ouahab, L. *Chem. Commun.* **2001**, 849. (h) Fortunelli, A.; Leoni, P.; Marchetti, L.; Pasquali, M.; Sbrana, F.; Selmi, M. *Inorg. Chem.* **2001**, *40*, 3055.

(10) μ-PCy_2: Leoni, P.; Marchetti, F.; Pasquali, M.; Marchetti, L.; Albinati, A. *Organometallics* **2002**, *21*, 2176.

(11) (a) Alonso, E.; Forniés, J.; Fortuño, C.; Martín, A.; Orpen, A. G. *Chem. Commun.* **1996**, 231. (b) Alonso, E.; Forniés, J.; Fortuño, C.; Martín, A.; Orpen, A. G. *Organometallics* **2000**, *19*, 2690. (c) Alonso, E.; Forniés, J.; Fortuño, C.; Martín, A.; Orpen, A. G. *Organometallics* **2001**, *20*, 850. (d) Brunner, H.; Dormeier, S.; Grau, I.; Zabel, M. *Eur. J. Inorg. Chem.* **2002**, 2603. (e) Alonso, E.; Forniés, J.; Fortuño, C.; Martín, A.; Orpen, A. G. *Organometallics* **2003**, *22*, 2723.

(12) (a) Alonso, E.; Forniés, J.; Fortuño, C.; Tomas, M. *J. Chem. Soc., Dalton Trans.* **1995**, 3777. (b) Alonso, E.; Casas, J. M.; Forniés, J.; Fortuño, C.; Martín, A.; Orpen, A. G.; Tsipis, C. A.; Tsipis, A. C. *Organometallics* **2001**, *20*, 5571.

Scheme 2

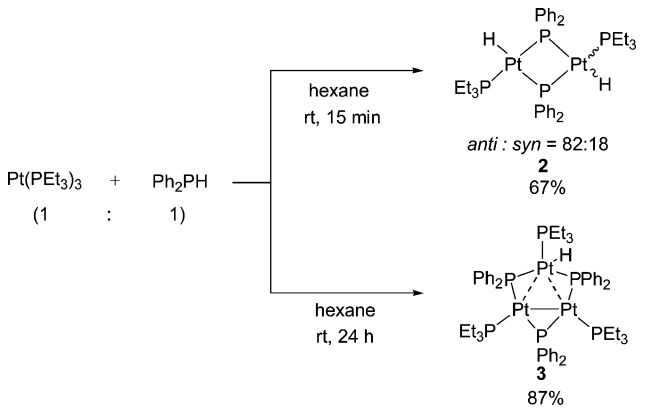

of PEt_3 of the bridging PPh_2 ligands are observed at δ 18.6 (^2J(P−P) = 308 Hz, ^1J(P−Pt) = 2294 Hz) and δ −105.9 and −118.6, respectively. The peak positions of the PPh_2 ligands are out of the range of the PPh_2 ligand which is bonded to the two metals, having a metal−metal bond (δ > 50).[3b,4a,12a,13] The signal pattern was complicated due to the presence of the isotopomers of the Pt centers and was characterized by comparison of the spectrum with that simulated based on an AA′BB′M-M′XX′X″ spin system, where AA′, BB′, MM′, and XX′X″ denote ^{31}P nuclei of the PPh_2 ligands *trans* to PEt_3 and those *cis* to PEt_3, PEt_3 ligands, and ^{195}Pt nuclei, respectively. The smaller signals of the *syn* isomer are severely overlapped with those of the *anti* isomer, and the precise peak positions and coupling constants were not determined.

Equimolar reactions of Ph_2PH with $Pt(PEt_3)_3$ at room temperature produce the dinuclear platinum(II) complex $[Pt_2H_2(\mu\text{-}PPh_2)_2(PEt_3)_2]$ (**2**) in 67% yield after 15 min and the triangular complex $[Pt_3H(\mu\text{-}PPh_2)_3(PEt_3)_3]$ (**3**) in 87% yield after 24 h, respectively, as shown in Scheme 2. The ^{1}H NMR data of **2** indicate the presence of *anti* and *syn* isomers in 82:18 ratio, similarly to the previously reported authentic sample.[14]

An ORTEP view of complex **3** projected onto the plane of the Pt_3 triangle is shown in Figure 2, while selected bond lengths and angles are listed in Table 2. The three Pt centers form an equilateral triangle with the Pt−Pt bond distances Pt(1)−Pt(2) = 2.9929(4) Å, Pt(1)−Pt(3) = 2.9784(4) Å, and Pt(2)−Pt(3) = 2.9983(3) Å. These distances are longer than those observed in platinum metal (2.774 Å)[9b,15] and in the range reported for triangular platinum complexes with Pt−Pt bonds.[9a,c,e,16] All three edges of the triangle are bridged by μ-PPh_2 ligands with bond distances of Pt−P = 2.242(2)−2.244(2) Å and bond angles of Pt−P−Pt = 82.25(6)−82.73(6)°. The six P atoms of the PEt_3 and PPh_2 ligands are included in the Pt_3 plane with a deviation smaller than 0.19 Å from the plane. The hydrido ligand is located at a distance of 1.4(1) Å from the Pt center. The distances and angles of the Pt−P bonds around this Pt center are similar to the other bond parameters of the

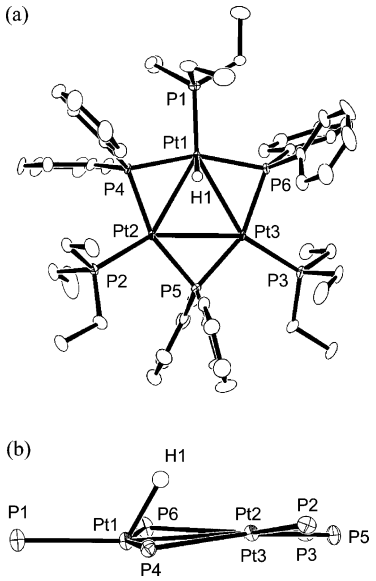

Figure 2. (a) ORTEP drawing (top view) of **3**·Ph_2PH with 50% thermal ellipsoidal plots. Hydrogen atoms except for Pt-H and Ph_2PH were omitted for simplicity. (b) Side view of **3**·Ph_2PH. Only Pt and P atoms and hydrido are shown.

complex. Thus, complex **3** is a 46e-trinuclear platinum complex, containing two Pt(I) and one Pt(II) center. Braunstein found two crystallographic structures of the 44e complex with two Pt(I) and one Pt(II) centers, $[Pt_3(Ph)(\mu\text{-}PPh_2)_3(PPh_3)_2]$.[9e] The structures with "an open form" had two shorter Pt−Pt bonds (2.758(3) Å) than the other (3.586(2) Å), whereas "a closed form" with three similar Pt−Pt bond lengths (2.956(3) and 3.074-(4) Å) was observed as the crystal structures of the same complex from different solvents. The geometry of **3** is comparable with the latter structure with three similar Pt−Pt distances.

The IR peak of **3** due to Pt−H stretching is observed at 2035 cm^{-1}, which suggests the nonbridging coordination of the hydride to a Pt center. The ^{1}H NMR spectrum of **3** shows the hydrido signal at δ −7.98 as a doublet (^2J(H−P) = 26 Hz) of triplets (^2J(H−P) = 66 Hz) with ^{195}Pt satellites (^1J(H−Pt) = 899 Hz), indicating that the hydrido ligand is bonded to one of the three Pt centers in solution. The coupling constant between the hydrido and the P nucleus of PEt_3 (26 Hz) is in the range of $PtH(PEt_3)L_n$ complexes[17] with H and PEt_3 ligands at *cis* positions (^2J(H−P) = 14−30 Hz) and much smaller than those of the complexes with the two ligands at *trans* positions (150−162 Hz). The actual H−Pt−PEt_3 bond angle in the solid state was determined as 117-(4)° by X-ray crystallography. Figure 3 shows the

(13) (a) Forniés, J.; Fortuño, C.; Navarro, R.; Martínez, F.; Welch, A. J. *J. Organomet. Chem.* **1990**, *394*, 643. (b) Falvello, L. R.; Forniés, J.; Fortuño, C.; Martín, A.; Martínez-Sariñena, A. P. *Organometallics* **1997**, *16*, 5849.

(14) (a) Chatt, J.; Davidson, J. M. *J. Chem. Soc.* **1964**, 2433. (b) Eaborn, C.; Odell, K. J.; Pidcock, A. *J. Organomet. Chem.* **1979**, *170*, 105.

(15) (a) Teatum, E. T.; Gschneider, K. A., Jr.; Waber, J. T. 1968 Compilation of Calculated Data Useful in Predicting Metallurgical Behavior of the Elements in Binary Alloy Systems; USAEC Report LA-4003, 1968 (supersedes Report LA-2345, 1960). (b) Bender, R.; Braunstein, P.; Jud, J. M.; Dusausoy, Y. *Inorg. Chem.* **1984**, *23*, 4489.

(16) (a) Green, M.; Howard, J. A. K.; Murray, M.; Spencer, J. L.; Stone, F. G. A. *J. Chem. Soc., Dalton Trans.* **1977**, 1509. (b) Evans, D. G.; Hughes, G. R.; Mingos, D. M. P.; Basset, J.-M.; Welch, A. J. *J. Chem. Soc., Chem. Commun.* **1980**, 1255. (c) Farrugia, L. J. Howard, J. A. K.; Mitrprachachon, P.; Stone, F. G. A.; Woodward, P. *J. Chem. Soc., Dalton Trans.* **1981**, 1134. (d) Scherer, O. J.; Konrad, R.; Guggolz, E.; Ziegler, M. L. *Chem. Ber.* **1985**, *118*, 1. (e) Ferguson, G.; Lloyd, B. R.; Puddephatt, R. J. *Organometallics* **1986**, *5*, 344. (f) Bott, S. G.; Hallam, M. F.; Ezomo, O. J.; Mingos, D. M. P.; Williams, I. D. *J. Chem. Soc., Dalton Trans.* **1988**, 1461.

Table 1. Analytical Results of Complexes[a]

complex	C (%)		H (%)	
$[Pt_3H_2(\mu\text{-}PPh_2)_4(PEt_3)_2]$ (**1**)	46.37	(46.70)	4.86	(4.73)
$[Pt_3H(\mu\text{-}PPh_2)_3(PEt_3)_3]$ (**3**)	43.59	(43.35)	4.88	(5.12)
$[Pt_2H_2(\mu\text{-}P^tBu_2)_2(PEt_3)_2]$ (**4**)	36.39	(36.60)	7.22	(7.46)
$[Pt_3(SiPh_3)(\mu\text{-}PPh_2)_3(PEt_3)_2]$ (**5**)	48.44	(48.44)	4.41	(4.62)
$[Pt_3(SiHPh_2)(\mu\text{-}PPh_2)_3(PEt_3)_2]$ (**6**)	46.52	(46.18)	4.65	(4.59)
$[Pt_3(\mu\text{-}PPh_2)_3(PEt_3)_3]^+I^-$ (**7**)[b]	39.85	(39.98)	4.40	(4.66)
$[Pt_3(\mu\text{-}PPh_2)_3(PEt_3)_3]^+[B_4O_4(C_6H_4Me\text{-}4)_4(OH)]^-$ (**8**)	49.91	(49.64)	5.41	(5.28)
$[Pt_3(\mu\text{-}PPh_2)_3(PEt_3)_3]^+[B_4O_4(C_6H_4F\text{-}4)_4(OH)]^-$ (**9**)	46.50	(46.84)	4.68	(4.64)
$[Pt_3(\mu\text{-}PPh_2)_3(PEt_3)_3]^+[B_4O_4(C_6H_4CF_3\text{-}4)_4(OH)]^-$ (**10**)	44.77	(44.42)	4.22	(4.37)

[a] Calculated values are shown in parentheses. [b] I; 8.05 (7.82).

Table 2. Selected Bond Distances (Å) and Angles (deg) of Complexes 3 and 5−8

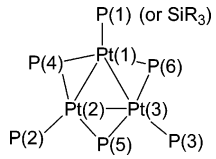

	3 (neutral, 46e)	**5** (neutral, 44e)	**6** (neutral, 44e)	**7** (cationic, 44e)	**8** (cationic, 44e)
Pt(1)−Pt(2)	2.9929(4)	3.0680(2)	2.9709(3)	3.0085(4)	3.0149(3)
Pt(1)−Pt(3)	2.9784(4)	3.0413(3)	3.0090(2)	3.0140(3)	3.0309(3)
Pt(2)−Pt(3)	2.9983(3)	3.0035(2)	3.0992(3)	3.0001(5)	3.0053(5)
Pt(1)−P(1) or Si(1)	2.242(2)	2.314(2)	2.313(1)	2.249(1)	2.258(2)
Pt(2)−P(2)	2.244(2)	2.239(1)	2.237(1)	2.242(2)	2.254(2)
Pt(3)−P(3)	2.244(2)	2.244(2)	2.286(1)	2.242(2)	2.247(2)
Pt(2)−Pt(1)−Pt(3)	60.281(9)	58.892(5)	62.430(6)	59.755(9)	59.613(8)
Pt(1)−Pt(2)−Pt(3)	59.621(9)	60.109(5)	59.387(6)	60.215(9)	60.459(8)
Pt(1)−Pt(3)−Pt(2)	60.099(9)	60.999(5)	58.183(6)	60.030(9)	59.928(8)
Pt(1)−P(4)−Pt(2)	82.25(6)	85.31(6)	81.54(4)	82.54(7)	82.99(6)
Pt(1)−P(6)−Pt(3)	82.32(6)	83.45(3)	82.82(4)	82.83(7)	83.33(7)
Pt(2)−P(5)−Pt(3)	82.73(6)	82.84(5)	86.02(4)	82.39(5)	82.55(5)

$^{31}P\{^1H\}$ NMR spectrum of **3** and a simulated spectrum based on the structure. Two signals assigned to the μ-PPh_2 ligands were observed at δ −24.68 (^2J(P−P) = 147, 210 Hz, ^1J(P−Pt) = 1960, 2239 Hz) and 161.50 (^2J(P−P) = 15, 210 Hz, ^1J(P−Pt) = 2700 Hz) in a 2:1 peak area ratio. High magnetic field shift of the latter signal is attributed to the μ-PPh_2 ligand between the two Pt(I) centers bonded to each other.[9c,e−h,10,18] The two signals due to the PEt_3 ligands are observed at δ 13.64 (^2J(P−P) = 147 Hz, ^1J(P−Pt) = 2403 Hz) and 15.38 (^2J(P−P) = 15 Hz, ^3J(P−P) = −160 Hz, ^1J(P−Pt) = 2942 Hz, ^2J(P−Pt) = 502 Hz, ^3J(P−Pt) = 48 Hz) in approximately 1:2 peak area ratio. All the NMR results indicate that complex **3** has one Pt(II) and two Pt(I) centers and a certain Pt−Pt bond between the Pt(I) centers.

$Pt(PEt_3)_3$ reacts with $^tBu_2PH$ in benzene at 70 °C to produce the dinuclear platinum(II) complex $[Pt_2H_2(\mu\text{-}P^tBu_2)_2(PEt_3)_2]$ (**4**) in 72% isolated yield (eq 2). Figure

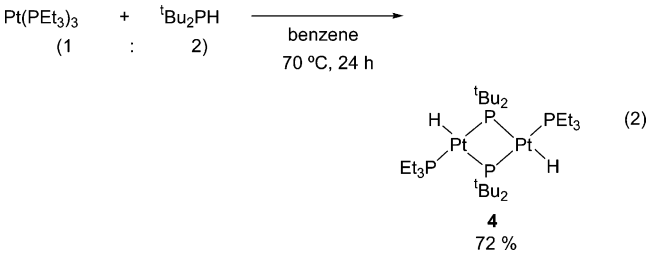

4 depicts the molecular structure of **4** established by X-ray crystallography. The two Pt centers are bridged by the μ-P^tBu_2 ligands and are bonded with the terminal PEt_3 ligands. Positions of the terminal hydrido ligands are not determined by X-ray diffraction. Between the two possible isomers of **4** which have the PEt_3 ligands at the same side or the opposite side of the Pt−Pt alignment, only the latter isomer was found in the crystallographic structures (*anti*).[19] Complex **4** shows a Pt(1)···Pt(1*) distance (3.646(1) Å) longer than that of the Pt−Pt bond of **1**. The bond angles P(2)−Pt(1)−P(2*) = 79.93(11)° and Pt(1)−P(2)−Pt(1*) = 100.07(11)° are slightly out of the range of the structural parameters of the reported phosphido-bridged platinum(II) dimers without a metal−metal bond (P−Pt−P 74.6−77.2°; Pt−P−Pt 102.8−105.4°).[5a,d,12] The Pt−PPh_2 bond *trans*

(17) (a) Barker, G. K.; Green, M.; Stone, F. G. A.; Welch, A. J.; Onak, T. P.; Siwapanyoyos, G. *J. Chem. Soc., Dalton Trans.* **1979**, 1687. (b) Barker, G. K.; Green, M.; Stone, F. G. A.; Welch, A. J.; Wolsey, W. C. *J. Chem. Soc., Chem. Commun.* **1980**, 627. (c) Almeida, J. F.; Dixon, K. R.; Eaborn, C.; Hitchcock, P. B.; Pidcock, A.; Vinaixa, J. *J. Chem. Soc., Chem. Commun.* **1982**, 1315. (d) Barker, G. K.; Green, M.; Stone, F. G. A.; Wolsey, W. C.; Welch, A. J. *J. Chem. Soc., Dalton Trans.* **1983**, 2063. (e) Cowan, R. L.; Trogler, W. C. *J. Am. Chem. Soc.* **1989**, *111*, 4750. (f) Litz, K. E.; Henderson, K.; Gourley, R. W.; Banaszak Holl, M. M. *Organometallics* **1995**, *14*, 5008. (g) Ara, I.; Berenguer, J. R.; Fornies, J.; Lalinde, E.; Moreno, M. T. *Organometallics* **1996**, *15*, 1820. (h) Han, L.-B.; Choi, N.; Tanaka, M. *Organometallics* **1996**, *15*, 3259. (i) Bender, J. E., IV; Litz, K. E.; Giarikos, D.; Wells, N. J.; Banaszak Holl, M. M.; Kampf, J. W. *Chem. Eur. J.* **1997**, *3*, 1793. (j) Koizumi, T.; Osakada, K.; Yamamoto, T. *Organometallics* **1997**, *16*, 6014. (k) Batten, S. A.; Jeffery, J. C.; Jones, P. L.; Mullica, D. F.; Rudd, M. D.; Sappenfield, E. L.; Stone, F. G. A.; Wolf, A. *Inorg. Chem.* **1997**, *36*, 2570. (l) Edelbach, B. L.; Lachicotte, R. J.; Jones, W. D. *J. Am. Chem. Soc.* **1998**, *120*, 2843. (m) Edelbach, B. L.; Vicic, D. A.; Lachicotte, R. J.; Jones, W. D. *Organometallics* **1998**, *17*, 4784. (n) Goodwin, A. A.; Bu, X.; Deming, T. J. *J. Organomet. Chem.* **1999**, *589*, 111.

(18) Brandon, J. B.; Dixon, K. R. *Can. J. Chem.* **1981**, *59*, 1188.

(19) The other isomer, *syn*, for $[Pt_2H_2(PCy_3H)_2(\mu\text{-}PCy_2)_2]$ was reported.[7]

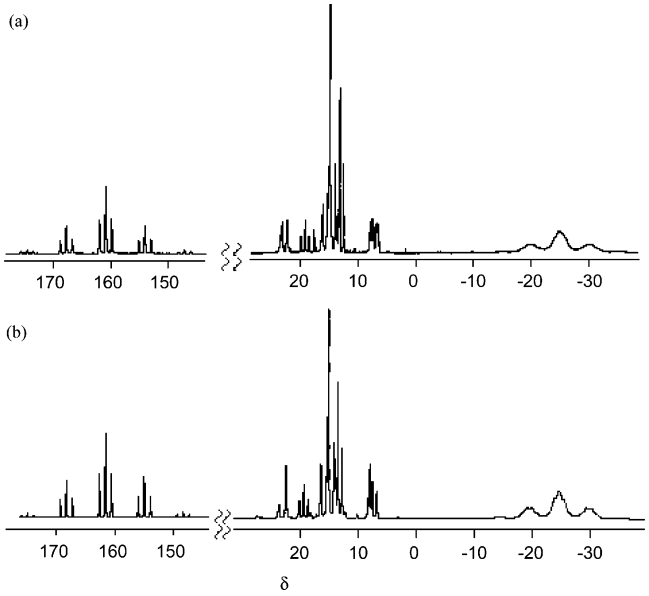

Figure 3. (a) Observed (CD_2Cl_2, rt) and (b) simulated $^{31}P\{^1H\}$ NMR spectra (202.4 MHz) of **3**.

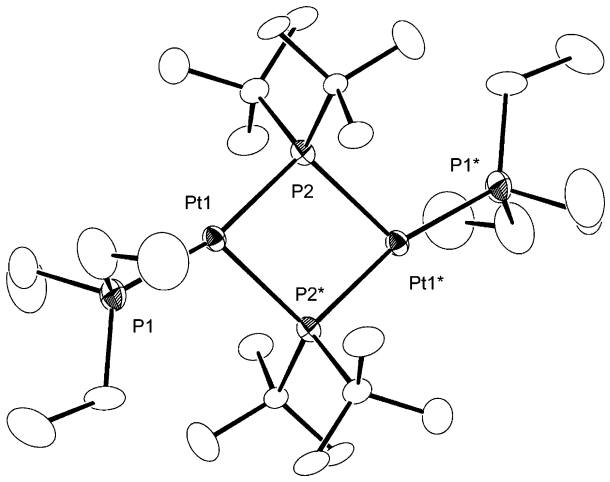

Figure 4. ORTEP drawing of **4** with 50% thermal ellipsoidal plots. Atoms with asterisks are crystallographically equivalent to those having the same number without asterisks. Hydrido ligands were not located. Hydrogen atoms were omitted for simplicity. Selected bond distances (Å) and angles (deg): Pt(1)−P(1) = 2.277(3), Pt(1)−P(2) = 2.345(3), Pt(1)−P(2*) = 2.412(3), Pt(1)···Pt(1*) = 3.646(1), P(2)···P(2*) = 3.056(6); P(1)−Pt(1)−P(2) = 166.01(12), P(1)−Pt(1)−P(2*) = 114.05(11), P(2)−Pt(1)−P(2*) = 79.93(11), Pt(1)−P(2)−Pt(1*) = 100.07(11).

to PEt_3 (2.345(3) Å) is shorter than the bond *trans* to the hydrido ligand (2.412(3) Å), suggesting that the hydrido ligand has stronger *trans* influence than PEt_3.

Complex **4** exhibits the IR band due to Pt−H stretching at 2022 cm^{-1}. The ^1H NMR signal of the hydrido ligand at δ −7.33 exhibits splitting due to H−P coupling. The coupling constant (151 Hz) being much larger than the other two coupling constants is assigned to that between the hydrido and μ-P^{t}Bu$_2$ ligand at *trans* positions. The coupling constant, ^1J(H−Pt), of 903 Hz is within those of the terminal hydrido ligand of diplatinum complexes (800−1400 Hz).[20] Figure 5 compares the observed and calculated $^{31}P\{^1H\}$ NMR spectra which contain resonances at δ 22.0 (^2J(P−P) = −20, −15, 285 Hz, ^1J(P−Pt) = 1972 Hz, ^3J(P−Pt) = 74 Hz) and −83.6

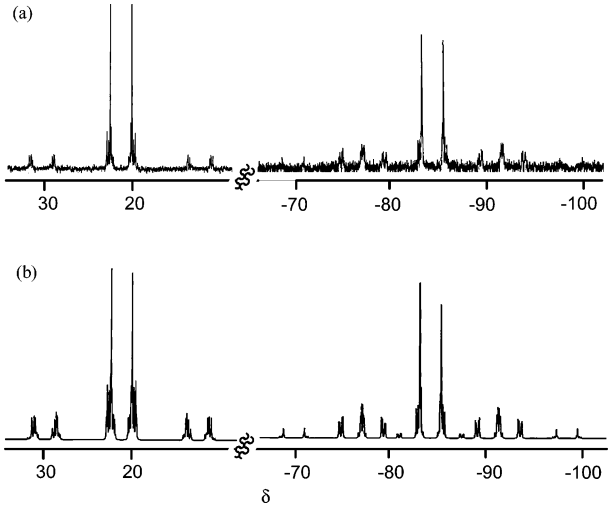

Figure 5. (a) Observed (C_6D_6, rt) and (b) calculated $^{31}P\{^1H\}$ NMR spectra (121.5 MHz) of **4**.

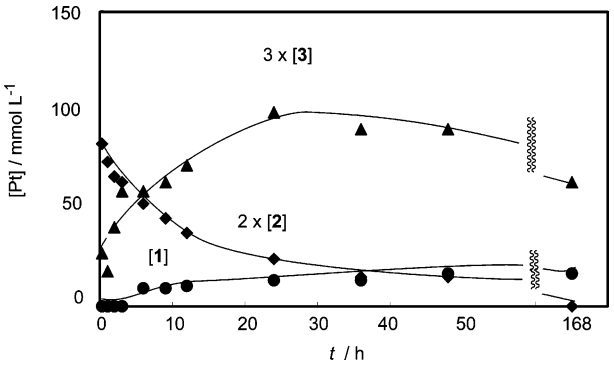

Figure 6. Profile of the amounts of Pt contained in the complexes during the reaction of Ph_2PH with $Pt(PEt_3)_3$ in an NMR tube scaled at 25 °C. [$Pt(PEt_3)_3$] = 160 mM at t = 0.

(^2J(P−P) = −15, 40, 285 Hz, ^1J(P−Pt) = 1496, 2016 Hz). The high-field signal at δ −83.6 is typical for the bridging phosphido ligand involved in the complexes without a Pt−Pt bond. All these NMR results indicate a symmetrical dimeric structure, in which two platinum atoms bearing a PEt_3 ligand are bridged by two P^{t}Bu$_2$ ligands.

Mechanism of Formation of 1. Complex **1** is formed also from the reaction of Ph_2PH with a mixture of **2** and $Pt(PEt_3)_3$ in 70% yield (eq 3). This reaction is enhanced

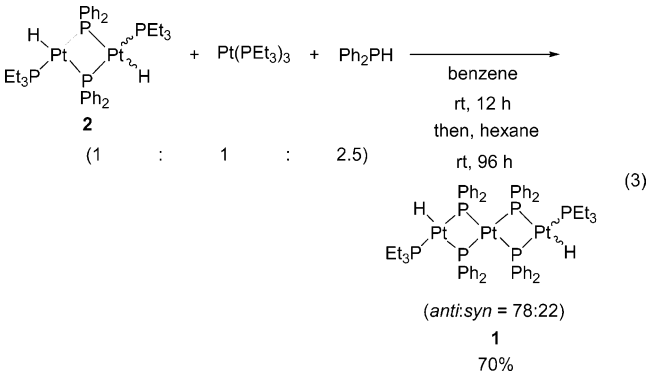

(3)

by removal of a free PEt_3 ligand under vacuum, which renders the replacement of the PEt_3 ligand by Ph_2PH facile. Figure 6 depicts a change of the amount of the

Scheme 3

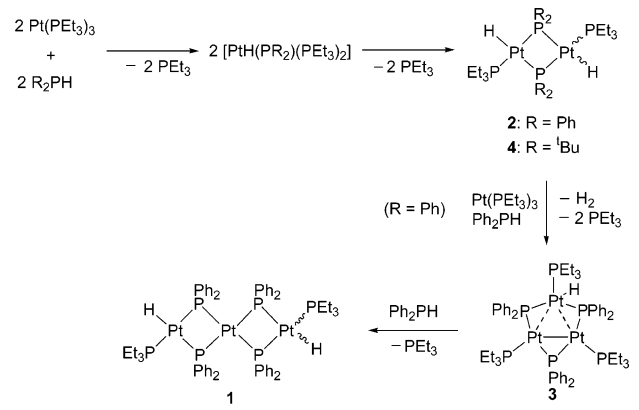

complexes monitored by the ^{1}H NMR spectra of the reaction mixture of Ph_2PH and $Pt(PEt_3)_3$ (2:1) at room temperature. The ^{1}H NMR spectrum after 20 min showed characteristic signals assigned to the hydrido ligands of **2** (δ −5.32) and **3** (δ −7.52), indicating the formation of the complexes in 55% and 18% yields, respectively. The $^{31}P\{^1H\}$ NMR spectrum of the reaction mixture measured at −70 °C and ESI-MS spectrum (*m*/*z* 997, calculated for $[Pt_2H(\mu\text{-}PPh_2)_2(PEt_3)_2]^+$; *m*/*z* 1494, calculated for $[Pt_3(\mu\text{-}PPh_2)_3(PEt_3)_3]^+$) also support the formation of **2** and **3** at this stage. Complex **3** increases concomitantly with a decrease of **2**, indicating conversion of **2** into **3** during the reaction. The initially formed **2** is consumed completely after 168 h, along with formation of **1**. In this reaction, removal of a free PEt_3 ligand under reduced pressure accelerates conversion of **3** into **1**. The 1:2 reaction of isolated complex **3** with Ph_2PH also produces **1** in 75% yield (eq 4). These results

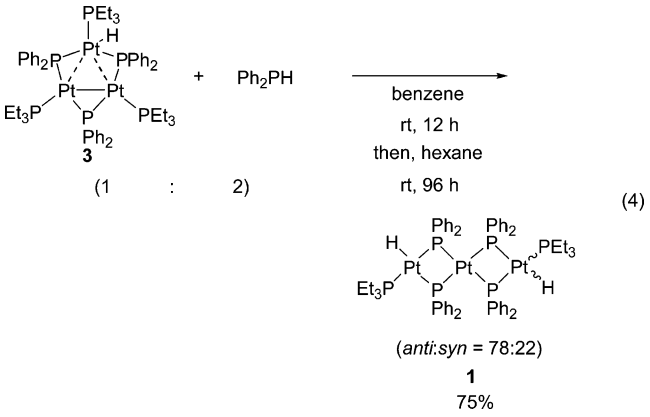

(4)

indicate that complexes **2** and **3** are formed as the intermediate of reaction 1.

A plausible reaction pathway for formation of dinuclear complexes **2** and **4** and trinuclear complexes **1** and **3** is shown in Scheme 3. Oxidative addition of R_2PH (R = Ph, ^{t}Bu) to $Pt(PEt_3)_3$ produces an intermediate Pt(II) complex, $[PtH(PPh_2)(PEt_3)_2]$, via cleavage of the P−H bond,[21] although this complex was not observed in the reaction mixture. Dimerization of the complex accompanied by elimination of PEt_3 leads to the dinuclear intermediate complex **2**. The reaction of ^{t}Bu$_2$PH with $Pt(PEt_3)_3$ produces **4** under more severe conditions (24 h at 70 °C) than that of Ph_2PH (15 min at room temperature) and does not give any trinuclear complexes. The sterically bulky ^{t}Bu substituent retards dimerization of $[PtH(P^tBu_2)(PEt_3)_2]$ into **4** and prevents formation of the linear trinuclear complex $[Pt_3H_2(\mu\text{-}P^tBu_2)_4(PEt_3)_2]$ with bridging di(*tert*-butyl)phosphido ligands. Complex **2** reacts further with $Pt(PEt_3)_3$ in the presence of Ph_2PH and/or with $[PtH(PPh_2)(PEt_3)_2]$ to form the triangular intermediate **3**. Evolution of H_2, which was detected by GC during reaction 1, takes place at this stage. Complex **3** reacts with Ph_2PH to form the linear complex **1** accompanied by liberation of PEt_3. Scheme 4 summarizes a mechanism of the reaction involving skeletal rearrangement of the Pt_3 unit. Replacement of a PEt_3 ligand of **3** with added Ph_2PH is followed by transfer of the P−H hydrogen of the ligand to the Pt(I) center bonded to the PEt_3 ligand. A cyclic intermediate **A**, formed by the reaction, undergoes bridging coordination of this PPh_2 ligand and rearrangement to the linear complex **1**, while another possible intermediate **B** undergoes bridging coordination of the two PPh_2 ligands to give **1**. Oxidative addition of Ph_2PH to the two Pt(I) centers of **3** is less plausible for the formation of these intermediates than reactions in Scheme 4 because formation of **1** in the reactions 1, 3, and 4 is accelerated by removal of PEt_3 from the solution under vacuum.

Reactions of 3 with Organosilanes and Arylboronic Acids. Complex **3** has a neutral and 46-electron structure composed of two Pt(I) and one Pt(II) center. The hydrido ligand of the triangular platinum complexes is much rarer[9b,h,10,22] than mono- and dinuclear hydridoplatinum complexes.[6b] We conducted the reactions of several organic molecules with **3**, expecting the formation of new triangular Pt complexes via the reaction of the Pt−H bond. The reactions of Ph_3SiH and of Ph_2SiH_2 with **3** afford $[Pt_3(SiPh_3)(\mu\text{-}PPh_2)_3(PEt_3)_2]$ (**5**) and $[Pt_3(SiHPh_2)(\mu\text{-}PPh_2)_3(PEt_3)_2]$ (**6**) in 75% and 82% yields, respectively (eq 5). The molecular structures of

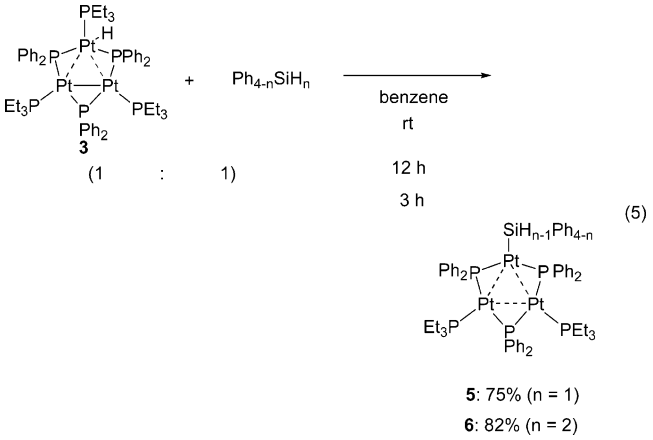

(5)

5 and **6** determined by X-ray crystallography are depicted in Figures7 and 8. The Pt−Pt bond distances of **5** are similar to those of $[Pt_3\{Si(OSiMe_3)_3\}(\mu\text{-}PPh_2)_3(PPh_3)_2]$, in which the Pt(I)−Pt(I) bond opposite the silyl ligand (3.0035(2) Å) is the shortest among the three Pt−Pt bond distances. Complex **6**, however, has a Pt(I)−Pt(I) bond (3.0992(3) Å) that is slightly longer than the Pt(I)−Pt(II) bond (2.9709(3) and 3.0090(2) Å). Steric repulsion between the phenyl rings of the μ-PPh_2 and of the $SiPh_3$ ligands renders the angle of Pt(2)−Pt(1)−Pt(3) smaller (58.892(5)°) than the corresponding bond angle of **6**, with the less bulky $SiHPh_2$ ligand

Scheme 4

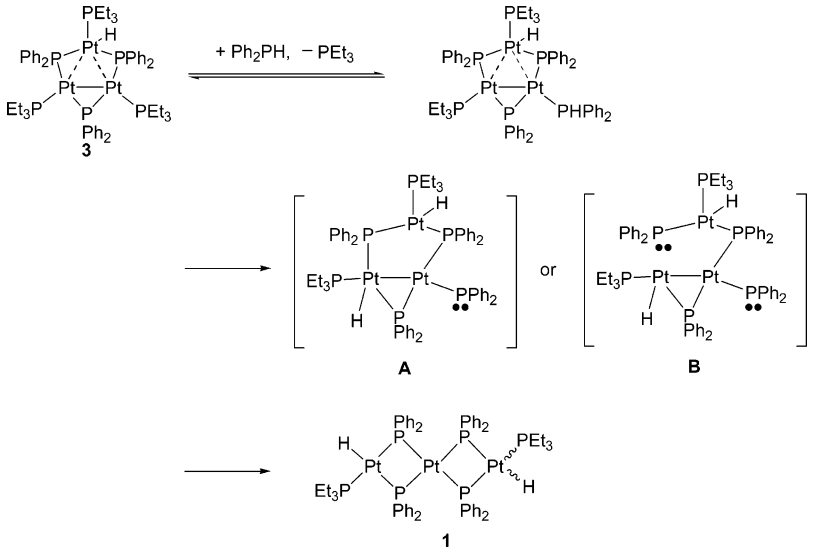

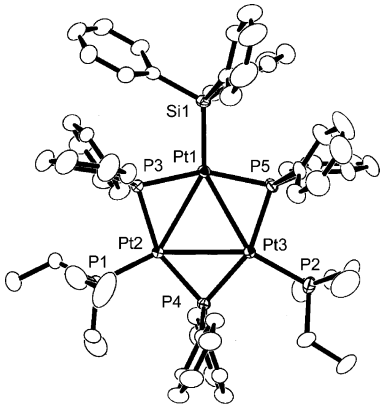

Figure 7. ORTEP drawing of **5** with 50% thermal ellipsoidal plots. Hydrogen atoms were omitted for simplicity.

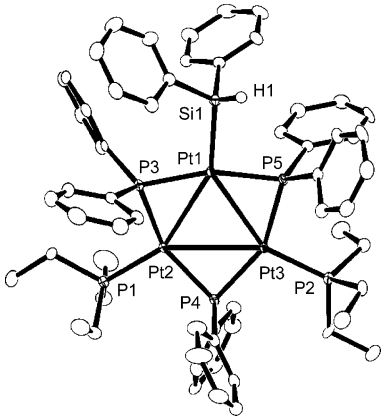

Figure 8. ORTEP drawing of **6** with 50% thermal ellipsoidal plots. Hydrogen atoms were omitted for simplicity.

(62.430(6)°). The Pt−P bond distances lie in the usual range, and the Pt−Si bonds (2.314(2) Å in **5** and 2.313(1) Å in **6**) are comparable to the single bond of the reported silylplatinum complexes.[23]

The ^{1}H NMR spectrum of **6** shows the signal of the Si−H hydrogen at δ 5.74 (^3J(H−P) = 10 Hz, ^3J(H−Pt) = 65 Hz, ^2J(H−Pt) = 170 Hz). The ^{31}P{^{1}H} NMR spectra of **5** and **6** contain three signals, corresponding to the terminal PEt_3 ligands (**5**, δ −7.68; **6**, δ −4.43) and to the chemically inequivalent phosphido ligands (**5**, δ 79.05 and 92.49; **6**, δ 79.96 and 91.73) in a 1:2 peak area ratio. All these signals are flanked by satellites due to a coupling with ^{195}Pt. Their formation could be explained by oxidative addition of the hydrosilanes to **3**, followed by reductive elimination of H_2 or, alternatively, by σ-bond metathesis. The latter mechanism would have the advantage of avoiding formal oxidation of the Pt(II) center in the mixed-valence complex **3**.

MeI was also employed to abstract the hydrido ligand of **3**.[24] An orange benzene solution of **3** quickly turned red upon addition of an equimolar amount of MeI. After the solution was stirred for 5 h at room temperature, $[Pt_3(\mu\text{-}PPh_2)_3(PEt_3)_3]^+I^-$ (**7**) was isolated as a dark red solid (eq 6). A perspective view of the molecular structure of **7** is shown in Figure 9, while the bond distances and angles are listed in Table 2. The cation has three Pt atoms arranged in an almost regular triangle, with Pt−Pt bond distances of Pt(1)−Pt(2) = 3.0085(4) Å, Pt(1)−Pt(3) = 3.0140(3) Å, and Pt(2)−Pt(3) = 3.0001-

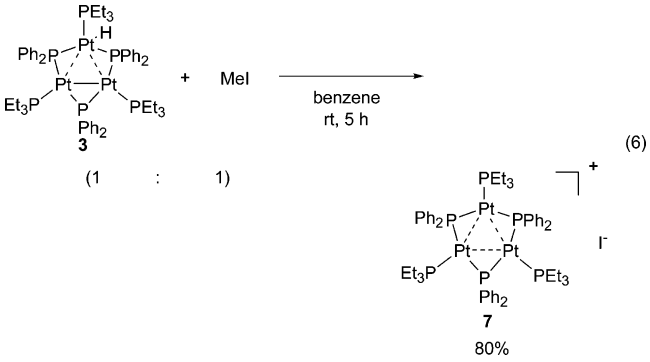

(6)

(20) (a) Brown, M. P.; Puddephatt, R. J.; Rashidi, M.; Seddon, K. R. *J. Chem. Soc., Dalton Trans.* **1978**, 516. (b) Bracher, G.; Grove, D. M. Venanzi, L. M.; Bachechi, F.; Mura, P.; Zambonelli, L. *Angew. Chem., Int. Ed. Engl.* **1978**, *17*, 778. (c) Morris, R. H.; Foley, H. C.; Targos, T. S.; Geoffroy, G. L. *J. Am. Chem. Soc.* **1981**, *103*, 7337. (d) Venanzi, L. M. *Coord. Chem. Rev.* **1982**, *43*, 251. (e) Moore, D. S.; Robinson, S. D. *Chem. Soc. Rev.* **1983**, *12*, 415. (f) Paonessa, R. S.; Troger, W. C. *J. Am. Chem. Soc.* **1982**, *104*, 3529. (g) Paonessa, R. S.; Trogler, W. C. *Inorg. Chem.* **1983**, *22*, 1038. (h) Bachechi, F.; Bracher, G.; Grove, D. M.; Kellenberger, B.; Pregosin, P. S.; Venanzi, L. M.; Zambonelli, L. *Inorg, Chem.* **1983**, *22*, 1031. (i) McLennan, A. J.; Puddephatt, R. J. *Organometallics* **1986**, 5, 811.

(5) Å. The Pt−Pt bonds are bridged by the phosphido ligands, with the P atoms lying approximately on the plane defined by the Pt atoms. Although a certain number of 44e$^-$ cationic triangular platinum species such as $[Pt_3(\mu\text{-}X)(\mu\text{-}PPh_2)_2(PPh_3)_3]^+$ (X = Cl, Br, SR, PPh_2) are known,[9d] complex **7**, to the best of our knowledge, is the first cationic Pt triangular derivative represented by the general formula $[Pt_3(\mu\text{-}L)_3(L')_3]^+$ (L = phosphido, L′ = phosphines) characterized by X-ray crystallography. The $^{31}P\{^1H\}$ NMR spectrum of **7** exhibits two signals at δ −2.65 (m, $^2J(P-P)$ = 63 Hz, $^1J(P-Pt)$ = 118, 4173 Hz) and δ 81.47 (m, $^2J(P-P)$ = −211 Hz, $^1J(P-Pt)$ = −103, 2246 Hz), indicating equivalency of all PEt_3 and μ-PPh_2 ligands.

One of the other synthetic protocols to obtain a cationic trinuclear platinum complex is protonation by a Brønsted acid. Leoni et al. reported that the neutral $[Pt_3(\mu\text{-}P^tBu_2)_3(H)(CO)_2]$ protonated with TfOH generated the cationic $[Pt_3(\mu\text{-}P^tBu_2)(\mu\text{-}H)(P^tBu_2H)(CO)_2]OTf$, along with migration of the μ-P^tBu_2 ligand into one of the Pt−H bonds.[9h] We have been engaged in studies of the reaction of weakly acidic arylboronic acid with Rh complexes to form novel Rh complexes with B-containing counteranions.[25] The reactions of 4 times molar arylboronic acids with **3** afforded the cationic platinum complexes $[Pt_3(\mu\text{-}PPh_2)_3(PEt_3)_3][B_4O_4(OH)Ar_4]$ (**8**, Ar = 4-methylphenyl; **9**, Ar = 4-fluorophenyl; **10**, Ar = 4-trifluoromethylphenyl) (eq 7). Complexes **8**−**10** were

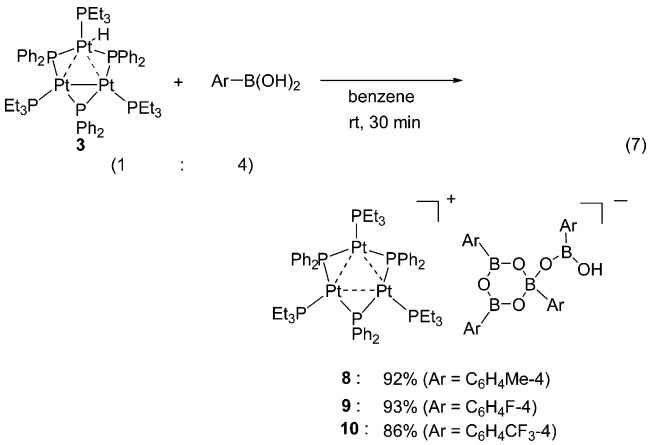

characterized by comparison of the NMR signals with those of **7** (^1H, $^{13}C\{^1H\}$, and $^{31}P\{^1H\}$), elemental analyses, and X-ray diffraction of **8**. An ORTEP drawing of **8** by X-ray diffraction is shown in Figure 10. The structure

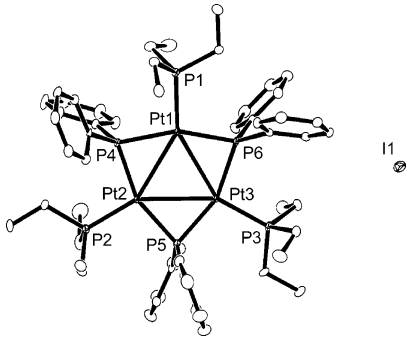

Figure 9. ORTEP drawing of **7**·CH_2Cl_2 with 50% thermal ellipsoidal plots. Hydrogen atoms and CH_2Cl_2 were omitted for simplicity.

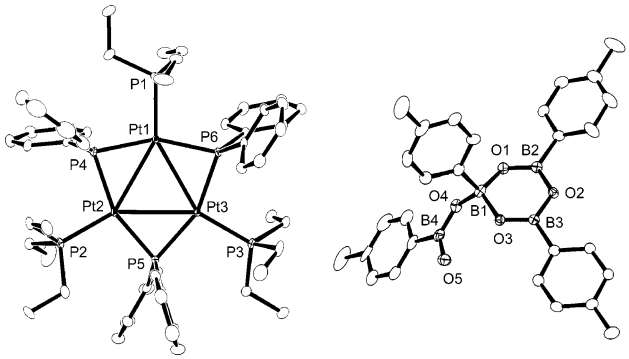

Figure 10. ORTEP drawing of **8** with 50% thermal ellipsoidal plots. Hydrogen atoms were omitted for simplicity. Selected bond distances (Å) and angles (deg): O(1)−B(1) = 1.45(1), O(1)−B(2) = 1.33(1), O(2)−B(2) = 1.393(8), O(2)−B(3) = 1.38(1), O(3)−B(1) = 1.513(8), O(3)−B(3) = 1.34(1), O(4)−B(1) = 1.48(1), O(4)−B(4) = 1.433(1), O(5)−B(4) = 1.37(1), C(55)−B(1) = 1.64(2); O(1)−B(1)−O(3) = 111.0(7), O(1)−B(1)−O(4) = 108.0(7), O(3)−B(1)−O(4) = 108.8(7), O(1)−B(2)−O(2) = 121.6(8), O(2)−B(3)−O(3) = 121.9(6), O(4)−B(4)−O(5) = 123.4(7), O(1)−B(1)−C(55) = 109.3(7), O(3)−B(1)−C(55) = 110.2(7), O(4)−B(1)−C(55) = 109.4(7).

of the cationic part of **8** is similar to that of **7**, while the anion part is composed of a novel tetraborate anion, $[B_4O_4(C_6H_4Me\text{-}4)_4(OH)]^-$, bearing a six-membered boroxine ring. The boroxine ring is almost flat due to pπ−pπ conjugation between filled p orbitals of oxygen and vacant p orbitals of boron.[26] The presence of a tetracoordinate boron atom of the B_3O_3 ring is observed; the B−O bonds of tetracoordinate boron (1.45(1)−1.513(8) Å) are longer than those observed in tricoordinate boron atoms (1.33(1)−1.393(8) Å). The two aryl planes are situated in parallel to a boroxine plane by the delocalization of the pπ orbitals of the boroxine and aryl rings. The ^{11}B NMR spectrum of **8** contains the two signals which are assigned to the tetracoordinate boron (δ 4.10) and tricoordinate boron (δ 28.12) nuclei in ca. 1:3 ratio. The ^1H, ^{11}B, and $^{31}P\{^1H\}$ NMR spectra of **9** and **10** are similar to those of **8**. An inorganic borate with a similar framework, $[B_4O_4(OH)_5]^-$, was detected as a product of the gas phase analysis of H_3BO_3 by negative CI mass spectra.[27] The anion of **8** is the first fully characterized anion with the $[B_4O_4(OH)X_4]^-$ framework.

Mechanism for Formation of 8−10. Scheme 5 depicts the plausible pathway for the formation of **8**−**10**. An arylboronic acid reacts with **3** to produce the cationic triplatinum complex and the arylboronate anion ac-

(21) (a) Pringle, P. G.; Smith, M. B. *J. Chem. Soc., Chem. Commun.* **1990**, 1701. (b) Hogarth, G.; Lavender, M. H. *J. Chem. Soc., Dalton Trans.* **1992**, 2759. (c) Baker, R. T.; Calabrese, J. C.; Harlow, R. L.; Williams, I. D. *Organometallics* **1993**, *12*, 830. (d) Han, L.-B.; Tanaka, M. *J. Am. Chem. Soc.* **1996**, *118*, 1571. (e) Wicht, D. K.; Kourkine, I. V.; Lew, B. M.; Nthenge, J. M.; Glueck, D. S. *J. Am. Chem. Soc.* **1997**, *119*, 5039. (f) Bourumeau, K.; Gaumont, A.-C.; Denis, J.-M. *J. Organomet. Chem.* **1997**, *529*, 205. (g) Costa, E.; Pringle, P. G.; Worboys, K. *Chem. Commun.* **1998**, 49. (h) Field, L. D.; Jones, N. G.; Turner, P. *J. Organomet. Chem.* **1998**, *571*, 195. (i) Dorn, H.; Jaska, C. A.; Singh, R. A.; Lough, A. J.; Manners, I. *Chem. Commun.* **2000**, 1041. (j) King, J. D.; Mays, M. J.; Mo, C.-Y.; Solan, G. A.; Conole, G.; McPartlin, M. *J. Organomet. Chem.* **2002**, *642*, 227.

(22) Pt−H (terminal): Leoni, P.; Mannetti, S.; F.; Pasquali, M.; Albinati, A. *Inorg. Chem.* **1996**, *35*, 6045.

(23) (a) Ebsworth, E. A. V.; Marganian, V. M.; Reed F. J. S.; Gould, R. O. *J. Chem. Soc., Dalton Trans.* **1978**, 1167. (b) Tilley, T. D. In *Transition-Metal Silyl Derivatives*; Patai, S., Rappoport, Z., Eds.; Wiley: New York, 1991; p 245. (c) Braunstein, P.; Knorr, M.; Hirle, B.; Reinhard G.; Schubert, U. *Angew. Chem., Int. Ed. Engl.* **1992**, *31*, 1583.

Scheme 5

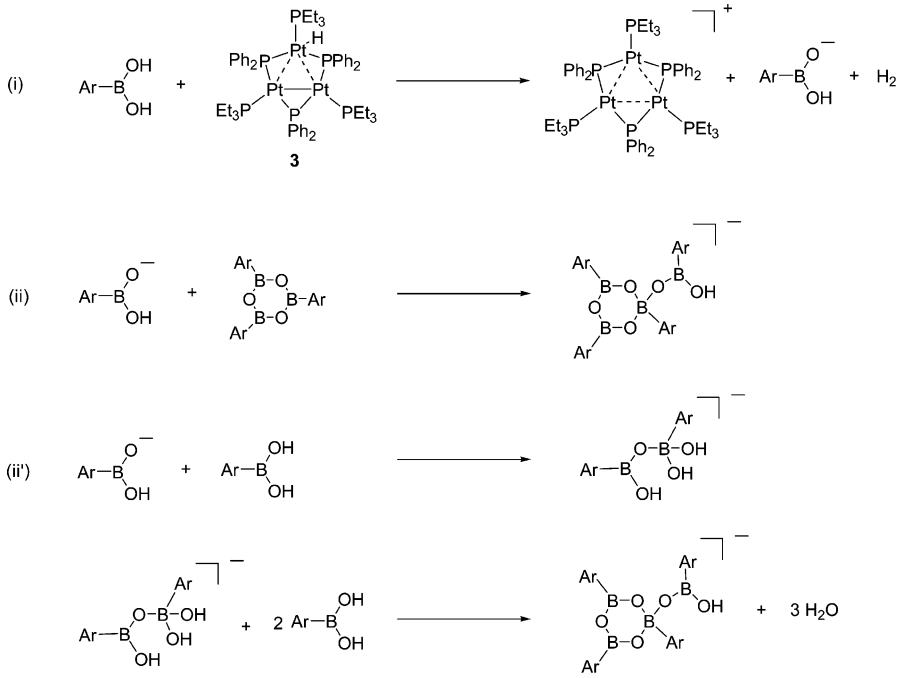

companied by liberation of H_2. Transfer of the borate to the electrophilic boron centers of arylboronic acid accompanied by cyclocondensation with two other arylboronic acid molecules or direct B−O bond formation between the borate and boroxine,[26a,b,d] which is equilibrated with the arylboronic acid via cyclocondensation, leads to the formation of $[B_4O_4(Ar)_4(OH)]^-$. An equimolar reaction of 4-methylphenylboronic acid with **3** produces **8** in 24% yield (by NMR) and unreacted **3**, indicating that the Pt-complex-promoted activation of the O−H bond in the added arylboronic acid is slower than the condensation of arylboronic acids toward arylboroxine or arylboronates.

In conclusion, this paper presents new di- or trinuclear phosphido-bridged platinum complexes with hydrido ligands and mechanistic implication of formation of the linear triplatinum complex, complex **3**, an intermediate of the formation of the linear trinuclear complex **1** upon addition of Ph_2PH. The Pt−H bond of **3** reacts with the Si−H bond of neutral Ph_3SiH and Ph_2SiH_2, the C−I bond of electrophilic MeI, and the O−H bond of weakly acidic arylboronic acid to produce the products with the respective new structures.

Experimental Section

General Procedures. All manipulations were carried out under a nitrogen or an argon atmosphere using standard Schlenk techniques. $Pt(PEt_3)_3$,[28] Ph_2PH,[29] and Ph_2PD[29] were prepared according to literature methods. NMR spectra (^1H, $^{13}C\{^1H\}$, and $^{31}P\{^1H\}$) were recorded on JEOL GX-500, JEOL EX-400, and Varian Mercury 300 spectrometers. Residual peaks of solvent were used as the reference for ^1H NMR (δ 5.32 dichloromethane-d_2, δ 7.15 benzene-d_6) and for $^{13}C\{^1H\}$ NMR (δ 53.8 dichloromethane-d_2, δ 128.0 benzene-d_6). $^{31}P\{^1H\}$ and ^{11}B NMR signals were referenced with external 85% H_3PO_4 (δ 0) and $BF_3{\cdot}OEt_2$ (δ 0), respectively. $^{19}F\{^1H\}$ NMR signals were referenced with internal $CFCl_3$ (δ 0). Elemental analyses were carried out with a Yanaco MT-5 CHN autocorder. The evolution of H_2 gas was analyzed by on-line gas chromatography (Shimadzu, GC-8A, TCD, molecular sieve 5 Å). The IR spectra were recorded on a Shimadzu FTIR-8100A spectrometer in KBr.

Preparation of $[Pt_3H_2(\mu\text{-}PPh_2)_4(PEt_3)_2]$ (1) (eq 1). To a benzene (15 mL) solution of $Pt(PEt_3)_3$ (560 mg, 1.0 mmol) was added Ph_2PH (348 μL, 2.0 mmol) at room temperature. The color of the solution turned from orange to red with stirring. After 12 h the volatiles were removed under reduced pressure. Addition of hexane (10 mL) to the resulting dark red oily materials and stirring for 96 h led to the formation of a yellow powder, which was filtered, washed with acetone (5 mL, 2 times), and dried in vacuo to give **1** as a yellow solid (426 mg, 0.27 mmol, 80% based on Pt, *anti*:*syn* = 78:22). Complex **1** crystallized from acetone at room temperature as yellow crystals. ^1H NMR (500 MHz, CD_2Cl_2, rt): δ −6.10 (ddd (*syn*) ^2J(H−P) = 11, 23, 142 Hz, ^1J(H−Pt) = 1036 Hz, 2H, Pt−*H*), −5.83 (ddd, (*anti*) ^2J(H−P) = 10, 22, 142 Hz, ^1J(H−Pt) = 1032 Hz, 2H, Pt−*H*), 0.84 (dt, (*anti*) ^3J(H−H) = 7 Hz, ^3J(H−P) = 17.0 Hz, 18H, PCH_2CH_3, overlapped *syn*), 1.24 (dq, (*anti*) ^3J(H−H) = 8 Hz, ^2J(H−P) = 8 Hz, 12H, PCH_2CH_3), 1.34 (dq, (*syn*), ^3J(H−H) = 8 Hz, ^2J(H−P) = 8 Hz, 12H, PCH_2CH_3), 6.79−7.30 (m, (*anti*) 40H, *Ph*, overlapped with *syn*). $^{31}P\{^1H\}$ NMR (202 MHz, CD_2Cl_2, rt): δ −118.6 ((*anti*), ^2J(P−P) = −19, 108, 200 Hz, ^1J(P−Pt) = 1232, 1273 Hz, ^3J(P−Pt) = 248 Hz, overlapped with *syn*), −105.9 ((*anti*), ^2J(P−P) = −19, 108, 300 Hz, ^1J(P−Pt) = 1807, 1935 Hz , ^3J(P−Pt) = 13 Hz, overlapped with *syn*), 18.6 ((*anti*), ^2J(P−P) = 308 Hz, ^1J(P−Pt) = 2294 Hz, overlapped with *syn*). IR (KBr): 1989 cm^{-1} (ν_{PtH}).

Preparation of $[Pt_2H_2(\mu\text{-}PPh_2)_2(PEt_3)_2]$ (2) (Scheme 1).[14] To a hexane (5 mL) solution of $Pt(PEt_3)_3$ (1.1 g, 2.0 mmol) was added Ph_2PH (360 μL, 2.0 mmol) at room temperature. The color of the solution turned from orange to red with stirring. The resulting red solution led to the formation of an orange solid with stirring for 15 min. After the sample was cooled at −20 °C, the resulting orange solid was filtered off and dried in vacuo to give **2** as an orange solid (668 mg, 67%, *anti*:*syn* = 82:18). ^1H NMR (500 MHz, toluene-d_8, rt): δ −6.13 (br, ^2J(H−P) = 198 Hz, ^1J(H−Pt) = 1034 Hz, 2H, Pt*H* (*syn*)), −5.69 (ddd, ^2J(H−P) = 47, 61, 198 Hz, ^1J(H−Pt) = 1046 Hz, 2H, Pt*H* (*anti*)), 0.88 (dt, ^3J(H−H) = 8 Hz, ^3J(H−P) = 16 Hz, 18H, PCH_2CH_3, (*anti*) overlapped with *syn*), 1.20 (m, ^3J(H−H) = 8 Hz, 12H, PCH_2CH_3 (*anti*)), 1.32 (br, 12H, PCH_2CH_3 (*syn*)), 6.94−7.10 (m, 12H, *Ph* (*anti*) overlapped with *syn*),

7.89 (m, 8H, *Ph* (*anti*) overlapped with *syn*). IR (KBr): 2004 cm^{-1} (ν_{PtH}).

Preparation of $[Pt_3H(\mu\text{-}PPh_2)_3(PEt_3)_3]$ (3) (Scheme 1). To a hexane (3 mL) solution of $Pt(PEt_3)_3$ (560 mg, 1.0 mmol) was added Ph_2PH (180 μL, 1.0 mmol) at room temperature. The color of the solution turned from orange to red with stirring. The resulting red solution led to the formation of an orange solid with stirring for 24 h. The solid product was collected by filtration and dried in vacuo to give **3** as an orange solid (440 mg, 87%). Dark red single crystals of **3** were obtained from the reaction mixture of Ph_2PH with $Pt(PEt_3)_3$ in 2:1 ratio in toluene-d_8. ^{1}H NMR (500 MHz, CD_2Cl_2, rt): δ −7.98 (dt, ^2J(H−P) = 26, 66 Hz, ^1J(H−Pt) = 899 Hz, 1H, Pt−*H*), 0.56 (dt, ^3J(H−H) = 8 Hz, ^3J(H−P) = 16 Hz, 18H, PCH_2CH_3), 1.03 (dt, ^3J(H−H) = 8 Hz, ^3J(H−P) = 16 Hz, 9H, PCH_2CH_3), 1.16 (dq, ^3J(H−H) = 8 Hz, ^2J(H−P) = 4 Hz, 12H, PCH_2CH_3), 1.40 (dq, ^3J(H−H) = 8 Hz, ^2J(H−P) = 8 Hz, 6H, PCH_2CH_3), 6.95−6.96 (m, 12H, *Ph*), 7.28−7.33 (m, 6H, *Ph*), 7.54−7.55 (m, 8H, *Ph*), 7.78 (m, 4H, *Ph*). ^{13}C{^{1}H} NMR (126 MHz, CD_2Cl_2, rt): δ 8.21 (s, ^3J(C−Pt) = 20 Hz, PCH_2CH_3), 9.15 (s, ^3J(C−Pt) = 26 Hz, PCH_2CH_3), 19.38 (m, ^1J(C−P) = 2, 10 Hz, ^2J(C−Pt) = 45 Hz, PCH_2CH_3), 20.23 (d, ^1J(C−P) = 29 Hz, ^2J(C−Pt) = 36 Hz, PCH_2CH_3), 126.12 (s, *Ph*-para), 126.43 (d, ^3J(C−P) = 8 Hz, *Ph*-meta), 127.73 (d, ^3J(C−P) = 10 Hz, *Ph*-meta), 127.79 (s, *Ph*-para), 133.14 (d, ^2J(C−P) = 13 Hz, ^3J(C−Pt) = 16 Hz, *Ph*-ortho), 135.82 (d, ^2J(C−P) = 12 Hz, ^3J(C−Pt) = 32 Hz, *Ph*-ortho), 141.65 (d, ^1J(C−P) = 19 Hz, ^2J(C−Pt) = 35 Hz, *Ph*-ipso), 147.94 (d, ^1J(C−P) = 18 Hz, *Ph*-ipso). ^{31}P{^{1}H} NMR (202 MHz, CD_2Cl_2, rt): δ −24.68 (br, ^2J(P−P) = 147, 210 Hz, ^1J(P−Pt) = 1960, 2239 Hz, μ-*P*Ph), 13.64 (t, ^2J(P−P) = 147 Hz, ^1J(P−Pt) = 2403 Hz, *P*Et_3), 15.38 (m, ^3J(P−P) = −160 Hz, ^2J(P−P) = 15 Hz, ^3J(P−Pt) = 48 Hz, ^2J(P−Pt) = 502 Hz, ^1J(P−Pt) = 2942 Hz, *P*Et_3), 161.50 (tt, ^2J(P−P) = 15, 210 Hz, ^1J(P−Pt) = 2700 Hz, μ-*P*Ph). IR (KBr): 2035 cm^{-1} (ν_{PtH}).

Preparation of $[Pt_2H_2(\mu\text{-}P^tBu_2)_2(PEt_3)_2]$ (4) (eq 2). To a benzene (10 mL) solution of $Pt(PEt_3)_3$ (550 mg, 1.0 mmol) was added ^{t}Bu_2PH (407 μL, 2.2 mmol) at room temperature. The resulting mixture was heated at 70 °C for 24 h, and the color of the solution turned from pale orange to orange with stirring. The volatiles were removed under reduced pressure. Addition of hexane (2 mL) to the resulting orange oily materials at −78 °C led to the formation of a pale yellow powder, which was washed with 2 mL of hexane (2 times) at −78 °C, collected by filtration, and dried in vacuo to give **4** as a pale yellow solid (331 mg, 0.36 mmol, 72%/based on Pt). Complex **4** crystallized from hexane at −20 °C as yellow crystals. ^{1}H NMR (500 MHz, C_6D_6, rt): δ −7.33 (ddd, ^2J(H−P) = 19, 23, 151 Hz, ^1J(H−Pt) = 903 Hz, PtH), 1.01 (dt, ^3J(H−P) = 8, 16 Hz, CH_3), 1.68 (d, ^4J(H−H) = 12 Hz, PEt_3), 1.71 (dq, ^2J(H−P) = 8, 8 Hz, CH_2). ^{31}P{^{1}H} NMR (122 MHz, C_6D_6, rt): δ −83.6 (^2J(P−P) = −15, 40, 285 Hz, ^1J(P−Pt) = 1496, 2016 Hz, μ-P^tBu_2), 22.0 (^2J(P−P) = −20, −15, 285 Hz, ^1J(P−Pt) = 74, 1972 Hz, PEt_3). ^{13}C{^{1}H} NMR (126 MHz, C_6D_6, rt): δ 9.32 (J(C−Pt) = 23 Hz), 22.43 (d, ^1J(C−P) = 25 Hz, ^2J(C−Pt) = 58 Hz), 33.83 (d, ^2J(C−P) = 6 Hz), 34.01 (d, ^1J(C−P) = 39 Hz). IR (KBr): 2022 cm^{-1} (ν_{PtH}).

Reaction of Ph_2PH with 2 and $Pt(PEt_3)_3$ (eq 3). To a benzene (5 mL) solution of $Pt(PEt_3)_3$ (110 mg, 0.2 mmol) were added $[Pt_2H_2(\mu\text{-}PPh_2)_2(PEt_3)_2]$ (**2**) (200 mg, 0.2 mmol) and Ph_2PH (86 μL, 0.5 mmol) at room temperature. The color of the solution turned from orange to red with stirring. After 12 h the volatiles were removed under reduced pressure. Addition of hexane (10 mL) to the resulting dark red oily materials led to the formation of a yellow powder with stirring at 96 h, which was filtered and washed with 5 mL of acetone (2 times), collected by filtration, and dried in vacuo to give **3** as a yellow solid (219 mg, 0.14 mmol, 70%).

Reaction of Ph_2PH with 2 (eq 4). To a benzene (5 mL) solution of **3** (225 mg, 0.15 mmol) was added Ph_2PH (27 μL, 0.3 mmol) at room temperature. The color of the solution turned from orange to red with stirring. After 12 h the volatiles were removed under reduced pressure. Addition of hexane (10 mL) to the resulting dark red oily materials led to the formation of a yellow powder with stirring at 96 h, which was filtered and washed with 5 mL of acetone (2 times), collected by filtration, and dried in vacuo to give **3** as a yellow solid (176 mg, 0.11 mmol, 75%).

Reaction of Ph_2PH with $Pt(PEt_3)_3$ on the NMR Scale (Figure 6). To a solution of $Pt(PEt_3)_3$ (55 mg, 0.1 mmol) in toluene-d_8 (0.6 mL) was added Ph_2PH (35 μL, 0.2 mmol) at room temperature. The ^{1}H NMR spectra were recorded over 168 h. The yields of complexes **1**−**3** were determined by ^{1}H NMR based on Pt using diphenylmethane (17 μL, 0.1 mmol) as an internal standard.

Preparation of $[Pt_3(SiPh_3)(\mu\text{-}PPh_2)_3(PEt_3)_2]$ (5) and $[Pt_3(SiHPh_2)(\mu\text{-}PPh_2)_3(PEt_3)_2]$ (6). To a benzene (3 mL) solution of **3** (150 mg, 0.1 mmol) was added Ph_3SiH (26.0 mg, 0.1 mmol) at room temperature. The color of the solution turned immediately from orange to red with stirring. After 12 h, the solvent was removed under reduced pressure. Addition of hexane (2 mL) to the resulting red residue at −78 °C led to the formation of an orange solid, which was washed with hexane (2 mL, 2 times), collected by filtration, and dried in vacuo to give **5** as an orange solid (123.5 mg, 0.075 mmol, 75%). Complex **5** crystallized from CH_2Cl_2−hexane at room temperature as dark red crystals suitable for X-ray analysis. ^{1}H NMR (500 MHz, CD_2Cl_2, rt): δ 0.38 (dt, ^3J(H−H) = 8 Hz, ^3J(H−P) = 16 Hz, 18H, PCH_2CH_3), 1.51 (dq, ^3J(H−H) = 8 Hz, ^3J(H−P) = 8 Hz, 12H, PCH_2CH_3), 6.72 (t, J(H−H) = 8 Hz, 6H, Si−*Ph*), 6.87−6.90 (m, 9H, Si−*Ph*), 6.94 (t, J(H−H) = 8 Hz, 8H, μ-P*Ph*), 7.05−7.13 (m, 12H, μ-P*Ph*), 7.23 (m, 2H, μ-P*Ph*), 7.29 (m, 4H, μ-P*Ph*), 7.75 (m, 4H, μ-P*Ph*). ^{13}C{^{1}H} NMR (126 MHz, CD_2Cl_2, rt): δ 7.91 (s, PCH_2CH_3), 18.70 (dd, PCH_2CH_3), 126.05 (s), 127.21 (m), 127.32 (br), 127.93 (m), 133.74 (dt, J = 13, 2 Hz), 133.94 (dt, J = 7, 2 Hz), 137.18 (s, J(C−Pt) = 23 Hz), 139.69 (dt, J = 18, 2 Hz), 140.24 (dt, J = 31, 2 Hz), 146.68 (s, J(C−Pt) = 66 Hz, *Ph*-ipso). ^{31}P{^{1}H} NMR (202 MHz, CD_2Cl_2, rt): δ −7.68 (m, ^1J(P−Pt) = 4133, ^2J(P−Pt) = 191 Hz, J(P−P) = 108 Hz, *P*Et_3), 79.05 (m, ^1J(P−Pt) = 2330, ^2J(P−Pt) = −70 Hz, ^2J(P−P) = 195 Hz, μ-*P*Ph_2), 92.49 (m, ^1J(P−Pt) = 2283, 2195 Hz, ^2J(P−Pt) = 147 Hz, ^2J(P−P) = 248, 195 Hz, μ-PPh_2).

$[Pt_3(SiHPh_2)(\mu\text{-}PPh_2)_3(PEt_3)_2]$ (**6**) was prepared analogously to **5** from the reaction of Ph_2SiH_2 (18.6 μL, 0.1 mmol) with **3** (150 mg, 0.1 mmol) for 3 h at room temperature (128.0 mg, 0.082 mmol, 82%). Complex **6** crystallized from CH_2Cl_2−hexane at room temperature as dark red crystals. ^{1}H NMR (500 MHz, CD_2Cl_2, rt): δ 0.44 (dt, ^3J(H−H) = 8 Hz, ^3J(H−P) = 16 Hz, 18H, PCH_2CH_3), 1.61 (dt, ^3J(H−H) = 8 Hz, ^3J(H−P) = 16 Hz, 12H, PCH_2CH_3), 5.74 (t, ^3J(H−P) = 10 Hz, ^3J(H−Pt) = 65 Hz, ^2J(H−Pt) = 170 Hz, 1H), 6.77 (t, J(H−H) = 8 Hz, 4H, *Ph*), 6.89−6.92 (m, 6H, *Ph*), 7.06 (t, J(H−H) = 8 Hz, 8H, *Ph*), 7.13 (m, 4H, *Ph*), 7.23 (m, 2H, Ph), 7.29 (m, 4H, Ph), 7.37−7.42 (m, 8H, Ph), 7.71−7.74 (m, 4H, Ph). ^{13}C{^{1}H} NMR (126 MHz, CD_2Cl_2, rt): δ 8.01 (s, PCH_2CH_3), 19.25 (t, ^2J(C−P) = 16 Hz, ^3J(C−Pt) = 64 Hz, PCH_2CH_3), 126.12 (s, *Ph*-para), 126.43 (d, ^3J(C−P) = 8 Hz, *Ph*-meta), 127.73 (d, ^3J(C−P) = 10 Hz, *Ph*-meta), 127.79 (s, *Ph*-para), 133.14 (d, ^2J(C−P) = 13 Hz, ^3J(C−Pt) = 16 Hz, *Ph*-ortho), 135.82 (d, ^2J(C−P) = 12 Hz, ^3J(C−Pt) = 32 Hz, *Ph*-ortho), 141.65 (d, ^1J(C−P) = 19 Hz, ^2J(C−Pt) = 35 Hz, *Ph*-ipso), 147.94 (d, ^1J(C−P) = 18 Hz, *Ph*-ipso). ^{31}P{^{1}H} NMR (202 MHz, CD_2Cl_2, rt): δ −4.43 (m, ^1J(P−Pt) = 4191 Hz, ^2J(P−Pt) = 188 Hz, *P*Et_3), 79.96 (m, ^1J(P−Pt) = 2379 Hz, ^2J(P−Pt) = −76 Hz, ^2J(P−P) = 199 Hz, μ-*P*Ph_2), 91.73 (m, ^1J(P−Pt) = 2203, 2216 Hz, ^2J(P−Pt) = 132 Hz, ^2J(P−P) = 240 Hz, μ-*P*Ph_2).

Preparation of $[Pt_3(\mu\text{-}PPh_2)_3(PEt_3)_3]^+I^-$ (7). To a benzene (2 mL) solution of **3** (150 mg, 0.1 mmol) was added MeI (6.25 μL, 0.1 mmol) at room temperature. The color of the solution turned immediately from orange to red with stirring. Stirring of the resulting red solution for 5 h led to separation of a brown solid, which was collected by filtration, washed with hexane

Table 3. Crystal Data and Details of the Structure Refinement of 1 and 3−8

	1	3	4
formula	$C_{60}H_{72}P_6Pt_3 \cdot Me_2CO$	$C_{54}H_{76}P_6Pt_3 \cdot Ph_2PH$	$C_{28}H_{68}P_4Pt_2$
molecular weight	1622.42	1682.50	918.92
cryst syst	triclinic	monoclinic	monoclinic
space group	$P\bar{1}$ (No. 2)	$P2_1/c$ (No. 14)	$P2_1/c$ (No. 14)
a (Å)	12.549(2)	12.866(2)	10.732(2)
b (Å)	13.145(2)	31.112(5)	15.903(3)
c (Å)	11.270(3)	18.060(3)	11.707(2)
α (deg)	94.12(1)	90	90
β (deg)	94.067(8)	109.847(2)	116.063(6)
γ (deg)	115.04(1)	90	90
V (Å^3)	1669.3(6)	6799.9(21)	1794.8(5)
Z	1	4	2
μ (mm^{-1})	6.425	6.333	7.948
F(000)	788	3288	904
D_{calcd} (g cm^{-3})	1.614	1.643	1.700
cryst size (mm)	0.15 × 0.12 × 0.07	0.61 × 0.59 × 0.57	0.23 × 0.18 × 0.12
2θ range (deg)	5.0−55.0	5.0−55.0	5.0−55.0
no. of unique reflns	6258	14 268	4047
no. of used reflns	4669	12 312	3195
no. of variables	390	787	187
R	0.063	0.043	0.049
R_w[a]	0.078	0.070	0.072
GOF	0.98	1.410	1.06

	5	6	7	8
formula	$C_{66}H_{75}P_5SiPt_3$	$C_{60}H_{71}P_5SiPt_3$	$C_{54}H_{75}IP_6Pt_3 \cdot CH_2Cl_2$	$C_{82}H_{104}B_4O_5P_6Pt_3$
molecular weight	1636.54	1560.45	1707.14	1984.07
cryst syst	triclinic	monoclinic	triclinic	triclinic
space group	$P\bar{1}$ (No. 2)	$P21/n$ (No. 14)	$P\bar{1}$ (No. 2)	$P\bar{1}$ (No. 2)
a (Å)	13.874(2)	15.325(2)	14.035(2)	16.302(2)
b (Å)	14.179(1)	18.498(3)	14.083(1)	17.107(2)
c (Å)	19.134(2)	20.097(3)	18.915(3)	19.010(3)
α (deg)	74.373(8)	90	72.418(7)	88.341(8)
β (deg)	75.470(7)	91.157(2)	85.439(9)	66.841(6)
γ (deg)	60.964(5)	90	61.155(6)	65.780(5)
V (Å^3)	3136.6(6)	5696.0(15)	3111.9(7)	4389.3(9)
Z	2	4	2	2
μ (mm^{-1})	6.832	7.519	7.469	4.905
F(000)	1588	3016	1636	1960
D_{calcd} (g cm^{-3})	1.733	1.819	1.822	1.501
cryst size (mm)	0.53 × 0.35 × 0.22	0.50 × 0.40 × 0.20	0.70 × 0.40 × 0.25	0.72 × 0.56 × 0.25
2θ range (deg)	5.0−50.0	5.0−55.0	5.0−55.0	5.0−55.0
no. of unique reflns	13 221	13 396	13 201	18 602
no. of used reflns	11 545	11 028	11 916	15 597
no. of variables	751	696	681	1005
R	0.038	0.032	0.036	0.039
R_w[a]	0.047	0.038	0.057	0.055
GOF	0.738	0.696	1.180	1.035

[a] Weighting scheme $[\sigma(F_o)^2]^{-1}$.

(2 mL, 2 times), and dried in vacuo to give **7** as a brown solid (129.9 mg, 0.080 mmol, 80%). Complex **7** crystallizes from CH_2Cl_2−hexane at room temperature as dark red crystals. ^{1}H NMR (500 MHz, CD_2Cl_2, rt): δ 0.39 (dt, J(H−H) = 8 Hz, J(H−P) = 17 Hz, 27H, PCH$_2$C*H*$_3$), 1.62 (m, J(H−H) = 8 Hz, 18H, PC*H*$_2$CH$_3$), 7.31−7.34 (m, 18H, *Ph*), 7.67 (m, 12H, *Ph*). ^{13}C{^{1}H} NMR (126 MHz, CD_2Cl_2, rt): δ = 7.87 (s, J(C−Pt) = 25 Hz, PCH$_2$*C*H$_3$), 18.7 (m, J(C−P) = 15 Hz, J(C−Pt) = 60 Hz, P*C*H$_2$CH$_3$), 128.55 (m, J(C−P) = 5 Hz, *Ph*-meta), 129.31 (s, *Ph*-para), 133.47 (ddd, J(C−P) = 2, 5, 9 Hz, *Ph*-ortho), 137.11 (ddd, J(C−P) = 2, 13, 24 Hz, *Ph*-ipso). ^{31}P{^{1}H} NMR (202 MHz, CD_2Cl_2, rt): δ −2.65 (m, J(P−P) = 63 Hz, J(P−Pt) = 118, 4173 Hz), 81.47 (m, J(P−P) = −211 Hz, J(P−Pt) = −103, 2246 Hz).

Preparation of [Pt$_3$(μ-PPh$_2$)$_3$(PEt$_3$)$_3$][B$_4$O$_4$(OH)Ar$_4$] (8, Ar = C$_6$H$_4$Me-4; 9, Ar = C$_6$H$_4$F-4; 10, Ar = C$_6$H$_4$CF$_3$-4). To a benzene (3 mL) solution of **3** (150 mg, 0.1 mmol) was added 4-methylphenylboronic acid (54.4 mg, 0.4 mmol) at room temperature. The color of the solution turned immediately from orange to red with stirring. After 30 min the solvent was removed under reduced pressure. Addition of hexane (5 mL) to the red residue at −78 °C led to the formation of a reddish brown solid, which was washed with hexane (5 mL, 5 times), collected by filtration, and dried in vacuo to give **8** as a reddish brown solid (182.5 mg, 0.092 mmol, 92%). Complex **8** crystallized from CH_2Cl_2−hexane at room temperature as dark red crystals. ^{1}H NMR (500 MHz, CD_2Cl_2, rt): δ 0.41 (dt, ^3J(H−H) = 8 Hz, ^3J(H−P) = 18 Hz, 27H, PCH$_2$C*H*$_3$), 1.63 (dq, ^3J(H−H) = 8 Hz, ^3J(H−P) = 8 Hz, 18H, PC*H*$_2$CH$_3$), 2.24 (s, 3H, Me), 2.35 (s, 3H, Me), 2.39 (s, 6H, Me), 6.95 (d, ^3J(H−H) = 8 Hz, 2H), 7.15 (d, ^3J(H−H) = 8 Hz, 2H), 7.21 (d, ^3J(H−H) = 8 Hz, 4H), 7.31−7.36 (m, 18H, Ph), 7. 51 (d, ^3J(H−H) = 8 Hz, 2H), 7.53 (s, 1H, OH), 7.67−7.71 (m, 12H), 7.88 (d, ^3J(H−H) = 8 Hz, 2H), 8.01 (d, ^3J(H−H) = 8 Hz, 4H). ^{11}B NMR (161 MHz, CD_2Cl_2): δ 4.10 (br, 1B), 28.12 (br, 3B). ^{13}C{^{1}H} NMR (126 MHz, CD_2Cl_2, rt): δ 7.92 (s, J(C−Pt) = 25 Hz, PCH$_2$*C*H$_3$), 18.78 (t, J(C−P) = 16 Hz, J(C−Pt) = 71 Hz, P*C*H$_2$CH$_3$), 21.32 (s, Me), 21.68 (s, Me), 21.77 (s, 2C, Me), 127.62 (s), 128.09 (s), 128.32 (s), 128.60 (t, J(C−P) = 5 Hz, *Ph*-meta), 129.39 (s, Ph-para), 131.60 (s), 133.51 (ddd, J(C−P) = 2, 5, 9 Hz, Ph-ortho), 133.88 (s, Ph-ipso), 134.96 (s), 135.15 (s), 137.17 (ddd, J(C−P) = 2, 13, 24 Hz, Ph-ipso), 138.82 (s, Ph-ipso), 139.80 (s, 2C, Ph-ipso). ^{31}P{^{1}H} NMR (202 MHz, CD_2Cl_2, rt): δ −2.63 (m, J(P−P) = 66 Hz, J(P−Pt) = 116, 4168 Hz, PEt$_3$), 81.56 (m, J(P−P) = −208 Hz, J(P−Pt) = −92, 2240 Hz, μ-PPh$_2$).

$[Pt_3(\mu\text{-}PPh_2)_3(PEt_3)_3][B_4O_4(OH)(C_6H_4F\text{-}4)_4]$ (**9**) was prepared analogously from the reaction of 4-fluorophenylboronic acid (56.0 mg, 0.4 mmol) with **3** (150 mg, 0.1 mmol) in benzene (3 mL) for 30 min at room temperature (186.5 mg, 0.093 mmol, 93%). Complex **9** crystallized from CH_2Cl_2−hexane at room temperature as dark red crystals. ^{1}H NMR (500 MHz, CD_2Cl_2, rt): δ 0.40 (dt, ^3J(H−H) = 8 Hz, ^3J(H−P) = 17 Hz, 27H, PCH_2CH_3), 1.62 (dq, ^3J(H−H) = 8 Hz, ^3J(H−P) = 8 Hz, 18H, PCH_2CH_3), 6.83 (t, ^3J(H−H) = 9 Hz, 2H), 6.99 (t, ^3J(H−H) = 9 Hz, 2H), 7.06 (m, 4H), 7.30−7.34 (m, 18H), 7.39 (s, 1H, OH), 7.60 (t, ^3J(H−H) = 8 Hz, 2H), 7.59−7.69 (m, 12H), 7.96 (t, ^3J(H−H) = 8 Hz, 2H), 8.10 (m, 4H). ^{11}B NMR (161 MHz, CD_2Cl_2, rt): δ 3.95 (br, 1B), 27.67 (br, 3B). ^{13}C{^{1}H} NMR (126 MHz, CD_2Cl_2, rt): δ 7.90 (s, J(C−Pt) = 22, 11 Hz, PCH_2CH_3), 18.76 (t, J(C−P) = 18 Hz, J(C−Pt) = 72 Hz, PCH_2CH_3), 113.28 (d, ^2J(C−F) = 19 Hz), 114.01 (d, ^2J(C−F) = 20 Hz), 114.31 (d, ^2J(C−F) = 20 Hz), 114.43 (d, ^2J(C−F) = 20 Hz), 128.60 (m, J(C−P) = 5 Hz, *Ph*-meta), 129.37 (s, *Ph*-para), 132.91 (d, ^3J(C−F) = 6 Hz), 133.52 (dd, J(C−P) = 5, 9 Hz, *Ph*-ortho), 136.86 (d, ^3J(C−F) = 7 Hz), 137.14 (d, ^3J(C−F) = 7 Hz), 137.17 (dd, J = 25,16 Hz, *Ph*-ipso), 137.27 (d, ^3J(C−F) = 8 Hz), 161.91 (d, ^1J(C−F) = 239 Hz), 164.46 (d, ^1J(C−F) = 245 Hz), 164.91 (d, ^1J(C−F) = 247 Hz), 164.94 (d, ^1J(C−F) = 246 Hz). ^{19}F{^{1}H} NMR (282 MHz, CD_2Cl_2, rt): δ −112.23 (m, 1F), −112.36 (m, 1F), −113.66 (m, 1F), −120.40 (m, 1F). ^{31}P{^{1}H} NMR (202 MHz, CD_2Cl_2, rt): δ −2.65 (m, J(P−P) = 2, 10, 66 Hz, J(P−Pt) = 117, 4168 Hz, PEt_3), 81.56 (m, J(P−P) = −206 Hz, J(P−Pt) = −99, 2234 Hz, μ-PPh_2).

$[Pt_3(\mu\text{-}PPh_2)_3(PEt_3)_3][B_4O_4(OH)(C_6H_4CF_3\text{-}4)_4]$ (**10**) was prepared from the reaction of 4-trifluoromethylphenylboronic acid (76.0 mg, 0.4 mmol) with **3** (150 mg, 0.1 mmol) in benzene (3 mL) for 30 min at room temperature (189 mg, 0.086 mmol, 86%). Complex **10** crystallized from CH_2Cl_2−hexane at room temperature as dark red crystals. ^{1}H NMR (500 MHz, CD_2Cl_2, rt): δ 0.40 (dt, ^3J(H−H) = 8 Hz, ^3J(H−P) = 16 Hz, 27H, PCH_2CH_3), 1.62 (dq, ^3J(H−H) = 8 Hz, ^3J(H−P) = 8 Hz, 18H, PCH_2CH_3), 7.30−7.33 (m, 19H, Ph overlapped OH), 7.42 (d, ^3J(H−H) = 8 Hz, 2H), 7.58 (d, ^3J(H−H) = 8 Hz, 2H), 7.66−7.68 (m, 16H), 7.81 (d, ^3J(H−H) = 8 Hz, 2H), 8.09 (d, ^3J(H−H) = 8 Hz, 2H),8.25 (d, ^3J(H−H) = 8 Hz, 4H). ^{11}B NMR (161 MHz, CD_2Cl_2, rt): δ 3.94 (br, 1B), 28.01 (br, 3B). ^{13}C{^{1}H} NMR (126 MHz, CD_2Cl_2, rt): δ 7.91 (s, J(C−Pt) = 28 Hz, PCH_2CH_3), 18.82 (t, ^2J(C−P) = 16 Hz, ^3J(C−Pt) = 71 Hz, PCH_2CH_3), 123.67 (q, ^3J(C−F) = 4 Hz), 124.00 (q, ^3J(C−F) = 4 Hz), 124.32 (q, ^3J(C−F) = 4 Hz), 125.12 (q, ^1J(C−F) = 272 Hz, 2C, CF_3), 125.26 (q, ^1J(C−F) = 272 Hz, CF_3), 125.77 (q, ^1J(C−F) = 271 Hz, CF_3), 127.26 (q, ^2J(C−F) = 32 Hz), 128.62 (t, J(C−P) = 5 Hz, Ph-meta), 129.40 (s, Ph-para), 130.98 (q, ^2J(C−F) = 32 Hz), 131.69 (s), 131.84 (q, ^2J(C−F) = 32 Hz), 133.56 (ddd, J = 9, 5, 2 Hz, Ph-ortho), 135.09 (s), 135.33 (s), 137.22 (ddd, J(C−P) = 24, 13, 2 Hz, ^2J(C−Pt) = 68 Hz, Ph-ipso), 140.61 (m), 142.26 (m). ^{19}F{^{1}H} NMR (282 MHz, CD_2Cl_2, rt): δ −62.00 (s, 3F), −62.65 (s, 3F), −62.78 (s, 6F). ^{31}P{^{1}H} NMR (202 MHz, CD_2Cl_2, rt): δ −2.67 (m, J(P−P) = 2, 10, 66 Hz, J(P−Pt) = 117, 4168 Hz, PEt_3), 81.60 (m, J(P−P) = −209 Hz, J(P−Pt) = −99, 2247 Hz, μ-PPh_2).

X-ray Diffraction. Single crystals of **1** and **3**−**8** were grown from acetone and CH_2Cl_2−hexane, respectively. Crystallographic data and details of refinement are summarized in Table 3. The crystals were sealed in glass capillary tubes and mounted on a Rigaku RAXIS imaging plate (**1**) and a Rigaku Saturn CCD (**3**−**8**) area detector with graphite-monochromated Mo Kα radiation. An empirical absorption correction was applied. The data were corrected for Lorentz and polarization effects. All calculations were performed using the CrystalStructure[30] crystallographic software package. The structure was solved by direct methods[31] and expanded using Fourier techniques.[32] All non-hydrogen atoms were refined with anisotropic thermal parameters, whereas all hydrogen atoms were located by assuming the ideal geometry and included in the structure calculation without further refinement of the parameters.[33]

Acknowledgment. This work was financially supported by a Grant-in-Aid for Scientific Research from the Ministry of Education, Science, Sports, Technology and Culture of Japan. We also thank Prof. Munetaka Akita (Tokyo Institute of Technology) for X-ray crystal analysis of **1** with the imaging plate.

Supporting Information Available: Table of crystallographic data and complete tables of non-hydrogen and selected hydrogen parameters, bond lengths and angles, calculated hydrogen atom parameters, anisotropic thermal parameters, and intermolecular contacts for **1** and **3**−**8**. This material is available free of charge via the Internet at http://pubs.acs.org.

OM034131V

(24) Paonessa, R. S.; Prignano, A. L.; Trogler, W. C. *Organometallics* **1985**, *4*, 647.
(25) Nishihara, Y.; Nara, K.; Osakada, K. *Inorg. Chem.* **2002**, *41*, 4090.
(26) (a) Yalpani, M.; Boese, R. *Chem. Ber.* **1983**, *116*, 3347. (b) Song, Z. Z.; Zhou, Z. Y.; Mak, T. C. W.; Wong, H. N. C. *Angew. Chem., Int. Ed. Engl.* **1993**, *32*, 432. (c) Beckett, M. A.; Strickland, G. C.; Varma, K. S.; Hibbs, D. E.; Hursthouse, M. B.; Malik, K. M. A. *J. Organomet. Chem.* **1997**, *535*, 33. (d) Beckett, M. A.; Brassington, D. S.; Owen, P.; Hursthouse, M. B.; Light, M. E.; Malik, K. M. A.; Varma, K. S. *J. Organomet. Chem.* **1999**, *585*, 7.
(27) Attina, M.; Cacace, F.; Occhiucci, G.; Ricci, A. *Inorg. Chem.* **1992**, *31*, 3114.
(28) (a) Muetterties, E. L.; Gerlach, D. H.; Kane, A. R.; Parshall, G. W.; Jesson, J. P. *J. Am. Chem. Soc.* **1971**, *93*, 3543. (b) Yoshida, T.; Matsuda, T.; Otsuka, S. *Inorg. Synth.* **1979**, *19*, 107.
(29) Aguiar, A. M.; Beisler, J.; Mills, A. *J. Org. Chem.* **1962**, *27*, 1001.
(30) *Crystal Structure 3.10*, Crystal Structure Analysis Package; Rigaku and Rigaku/MSC, 2000−2002.
(31) SIR92: Altomare, A.; Cascarano, G.; Giacovazzo, C.; Guagliardi, A.; Burla, M.; Polidori, G.; Camalli, M. *J. Appl. Crystallogr.* **1994**, *27*, 435.
(32) DIRDIF99: Beurskens, P. T.; Admiraal, G.; Beurskens, G.; Bosman, W. P.; de Gelder, R.; Israel, R.; Smits, J. M. M. *The DIRDIF-99 Program System*, Technical Report of the Crystallography Laboratory; University of Nijmegen: The Netherlands, 1999.
(33) *International Tables for X-ray Crystallography*; Kynoch: Birmingham, England, 1974; Vol. 4.